Chapter 19

High-Performance Supercapacitors Based on Ionic Liquids and a Graphene Nanostructure

Elaheh Kowsari

Additional information is available at the end of the chapter

http://dx.doi.org/10.5772/59201

1. Introduction

Climate change and the limited availability of fossil fuels have greatly affected the world's economy and ecology. With a fast-growing market for portable electronic devices and the development of hybrid electric vehicles, there has been an ever increasing and urgent demand for environmentally friendly high-power energy resources [1]. The production of electrochemical energy is under serious consideration as an alternative energy/power source, as long as the consumption of this energy is designed to be more sustainable and more environmentally friendly. Systems for electrochemical energy storage and conversion include batteries, fuel cells and electrochemical capacitors (ECs) [2]. Electrochemical capacitors (ECs) are known by different names such as ultracapacitors, EDLC, or super capacitors. These names were invented by different manufactures of the ECs. The trade name of the first commercial device made by Nippon Electric Company (NEC) was supercapacitors, but Pinnacle Research Institute (PRI) called the ECs ultracapacitors. Whatever the trade name of ECs, they all refer to a capacitor, which stores electrical energy in the interface between an electrolyte and a solid electrode. Because of the low capacitance values of the electrostatic capacitors, they are limited to low power applications or at most short term memory back-up supplies [3-7]. A large capacitance value and a high operating cell voltage are required for a supercapacitor to have good performance [8, 9]. Hence, the development of both novel electrode materials with increased capacitance, such as grapheme-based materials [10–16], and electrolytes with wider potential windows, such as ionic liquid electrolytes or organic electrolytes, is required to optimize the overall performance of the supercapacitor [17]. Carbide-derived carbons have been investigated for use as electrodes in EDLCs. High surface area carbon materials mainly include activated carbon [18,19], porous carbon [20], carbide-derived carbon [21], onion-like carbon, carbon aerogels [22], carbon nanotubes (CNTs) [23, 24], carbon shell [25], graphene

[26], and graphene quantum dots [27]. CNT, especially the single-walled carbon nanotube (SWCNT), has intrinsically excellent properties as an active material, such as high SSA, high conductivity, high flexibility, regular pore structures, and electrochemical stability. Woong et al. fabricated all-solid-state flexible SCs using CNTs, regular office papers, and ionic-liquid-based silica gel electrolyte [28]. Although CNTs possess high electrical conductivity and large SSA, CNT-based supercapacitors still cannot meet an acceptable performance, which is probably due to the observed contact resistance between the electrode and the current collector. Compared with traditional porous carbon materials, graphene has very high electrical conductivity, large surface area, and a profuse interlayer structure. Hence, graphene-based materials are hugely favourable for their application to EDLCs [29, 30]. The advent of new forms of carbon materials such as high quality graphene sheets (single layer to a few layers) with superior electrical properties have allowed for the development of new engineered carbons for energy storage [31-35]. Owing to their large in-plane conductivities, graphene films are expected to play a crucial role in the development of electrodes for a variety of energy applications such as photovoltaics [36-39] and supercapacitors [40]. These materials have recently been used in supercapacitor devices to replace conventional carbon electrodes and have shown very good performance [41-46].

Graphene has been found to exhibit exceptionally high thermal conductivity, electrical conductivity and strength. [47-49]

Another outstanding characteristic of graphene is its exceptionally high specific surface area of up to 2675 m^2/g. Most significantly, the intrinsic capacitance of graphene was recently found to be 21 $\mu F/ cm^2$, [50] which sets the upper limit of EDL capacitance for all carbon-based materials. This study asserts that graphene is the ideal carbon electrodematerial for EDL supercapacitors because it is capable of storing an EDL capacitance value of up to 550 F/g, provided the entire 2675m^2/g is fully utilized. Another advantage of graphene in a supercapacitor electrode is the notion that both major surfaces of a graphene sheet are exterior surfaces readily accessible by electrolyte [51]. For EDLCs, ionic liquids (ILs) [52], room temperature molten salts composed of organic cation (and anion) are widely considered the electrolyte of the future. Ionic liquids are solventless electrolytes with many properties that make them attractive for electrochemical energy storage: high chemical and thermal stability, negligible vapour pressure, a broad electrochemical stability potential window and an immense parameter space in terms of ion selection and resulting properties. The most popular ionic liquids are based on imidazolium and several salts with the 1-ethyl-3-methyl-imidazolium cation (EMI), which displays a cathodic stability of -1.8 V vs. NHE, and with such anions as BF_4,PF_6, $(CF_3SO_2)_2N$,CF_3SO_3, which in turn divergently affect the limit of the anodic window, the melting point and hence the conductivity of the ionic liquids were developed [53-55]. The compatibility is between graphene sheets and ionic liquids, which are significantly larger than the molecular sizes of aqueous and other organic liquid electrolytes.

In this chapter, the efficacy of ionic liquids in supercapacitors and the research lines for the design of advanced electrode materials and configurations for graphen and IL-based high-performance supercapacitors are reviewed and discussed.

2. Discussion

2.1. Operating principles of double-layer capacitors

2.1.1. Device configuration

An ES is a charge-storage device similar to batteries in design and manufacturing. As shown in Fig. 1, electrochemical capacitors (supercapacitors) consist of two electrodes separated by an ion permeable membrane (separator), and an electrolyte connecting both electrodes electrically. By applying a voltage to the capacitor, an electric double layer is formed at both electrodes, which has a positive or negative layer of ions deposited in a mirror image on the opposite electrode [56, 57]. The principles of a single-cell double-layer capacitor and an illustration of the potential drop at the electrode/electrolyte interface are shown in figure1.

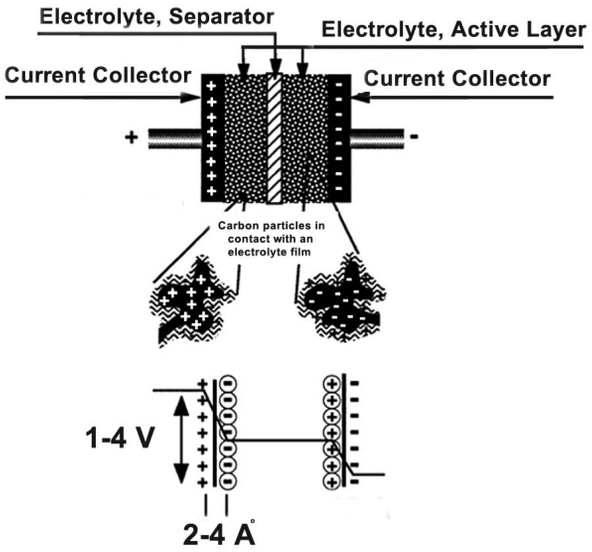

[Reprinted from [57] Kotz K, Carlen M. Principles and applications of electrochemical capacitors, Electrochim. Acta. 2000, 45, 2483-2498, Copyright (2000), with permission from Elsevier].

Figure 1. Principles of a single-cell double-layer capacitor and illustration of the potential drop at the electrode/electrolyte interface.

2.1.2. Capacitance distribution

The two electrodes form a series circuit of two individual capacitors C_1 and C_2. The total capacitance C_{total} is given by equation 1:

$$C_{total} = \frac{C_1.C_2}{C_1 + C_2} \tag{1}$$

Supercapacitors may have either symmetric or asymmetric electrodes. Symmetry implies that both electrodes have the same capacitance value. If $C_1 = C_2$, then $C_{total} = 0.5\ C_1$. For symmetric capacitors the total capacitance value equals half the value of a single electrode. For asymmetric capacitors, one of the electrodes typically has a higher capacitance value than the other. If $C_1 >> C_2$, then $C_{total} \approx C_2$. Thus, with asymmetric electrodes the total capacitance may be approximately equal to the smaller electrode [56, 57].

Ultracapacitors based on electrochemical double-layer capacitance (EDLC) are electrical energy storage devices that store and release energy by nanoscopic charge separation at the electrochemical interface between an electrode and an electrolyte. As the energy stored is inversely proportional to the thickness of the double layer, these capacitors have an extremely high energy density compared to conventional dielectric capacitors. This simple Helmholtz EDL model was further modified by Gouy and Chapman [58, 59] with the consideration of a continuous distribution of electrolyte ions (both cations and anions) in the electrolyte solution, driven by thermal motion, which is referred to as the diffuse layer. However, the Gouy–Chapman model leads to an overestimation of the EDL capacitance. The capacitance of two separated arrays of charges increases inversely with their separation distance, hence a very large capacitance value would arise in the case of point charge ions close to the electrode surface. Later, Stern [60] combined the Helmholtz model with the Gouy–Chapman model to explicitly recognize two regions of ion distribution, the inner region called the compact layer or the Stern layer and the diffuse layer [61, 62]. The structure of the electrolytic double layer and absorbed intermediates in electrode processes in aqueous solutions is shown in figure 2.

Research efforts have focused on increasing the energy and power densities of supercapacitors by increasing the surface area of porous electrodes and tailoring their morphology or pore size distribution [63]. Wang et al. presented general mathematical formulations for simulating electric double-layer capacitors (EDLCs) with three-dimensional ordered structures. A general set of boundary conditions was derived in order to account for the Stern layer without simulating it in the computational domain. These boundary conditions were valid for planar, cylindrical, and spherical electrode particles or pores. They conducted the simulations of EDLCs with as complex geometries as possible while rigorously accounting for both the Stern and diffuse layers. The model also simultaneously accounted not only for 3D electrode morphology but also for finite ion size and field-dependent electrolyte dielectric permittivity. It was used to faithfully simulate the complex structure of an EDLC electrode consisting of ordered bimodal mesoporous carbon, featuring both macropores and mesopores. Areal and gravimetric capacitances were predicted based on non-solvated and solvated ion diameters. These two cases set the upper and lower bounds for the predicted capacitances. The capacitances predicted using non-solvated ion diameter were found to be in good agreement with experimental data reported in the literature. All surfaces contributed to the overall capacitance of the EDLCs. The gravimetric capacitance of different bimodal carbons increased linearly with increasing specific surface area corresponding to constant areal capacitance.

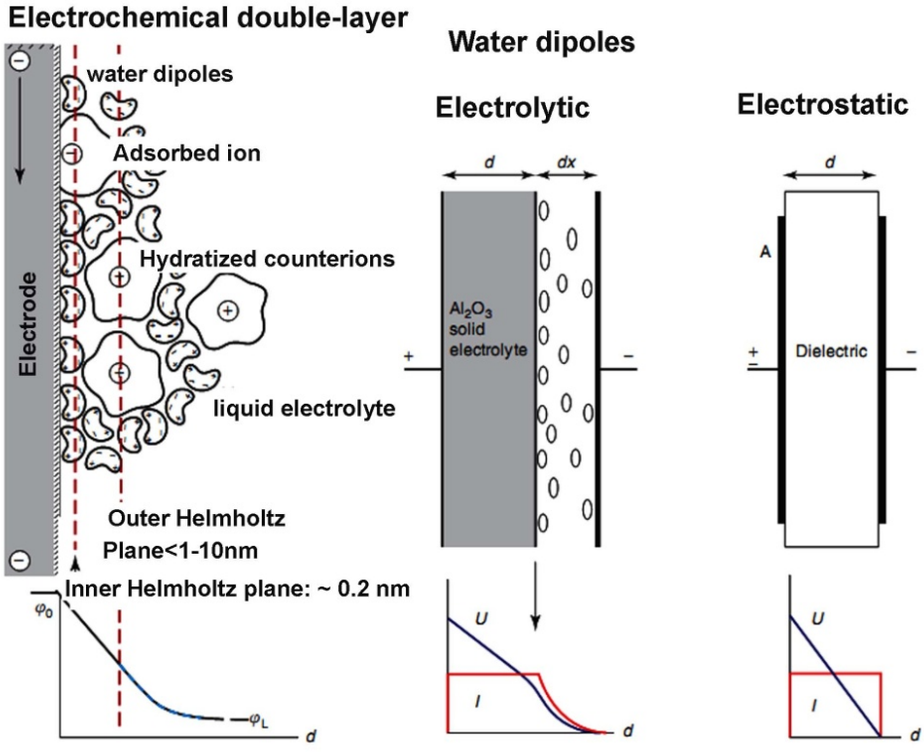

[Reprinted from [62] P. Kurzweil Capacitors | Electrochemical Double-Layer Capacitors, Reference Module in Chemistry, Molecular Sciences and Chemical Engineering Encyclopedia of Electrochemical Power Sources,2009, Pages 607–633, Copyright (2009), with permission from Elsevier].

Figure 2. Structure of the electrolytic double layer and absorbed intermediates in electrode processes in aqueous solutions. Below: potential profile through the rigid Helmholtz layer and the diffuse layer. Right: comparison of electrolytic and electrostatic capacitors.

2.2. State-of-the-art of constituent materials of a symmetrical carbon/carbon supercapacitor

2.2.1. Electrode

Static storage mechanisms in EDLCs efficiently store charges upon the electrodes at high rates. Unlike rechargeable batteries, ESs involves no chemical breakdown or redeposition of electrode materials during the operation. This lowers the risk of electrode phase changes during operation and enables long electrode cycle lives. The important requirements for the optimization of electrode materials include: minimal irreversible redox processes, high specific surface area, thermodynamic stability for a large potential window of operation, ability to control morphology, pore size, particle size, and material distribution, surface wettability, and high electrical conductivity.

The most suitable carbon structures used as active material for EDLC electrodes are: activated carbon, carbide derived carbon, onion-like carbons, carbon nanotubes and graphene. Carbon-based electrodes are of great interest as they are light-weight, of moderate cost, abundant, easy to process, possess high electronic conductivity and high specific surface area (high charge storage). A large surface area can be obtained owing to their versatility which enables the

different nanostructures to be produced, providing a wide variety of physical properties, to tailor for different types of applications.

2.2.1.1. Carbon materials for EDLC supercapacitors[1]

Activated Carbon (AC)

Activated carbon (AC) was the first material chosen for the EDLC electrodes. It has an electrical conductivity of 1,250 to 3,000 S/m, approximately 0.003% of metallic conductivity, but sufficient for supercapacitors [64,65].

Solid activated carbon, also called consolidated amorphous carbon (CAC), is the most used electrode material for supercapacitors and may be cheaper than other carbon derivatives. It is produced from activated carbon powder pressed into the desired shape, forming a block with a wide distribution of pore sizes. An electrode with a surface area of about 1000 m2/g results in a typical double-layer capacitance of about 10 μF/cm2 and a specific capacitance of 100 F/g. Activated carbon electrodes exhibit a predominantly static double-layer capacitance, but also exhibit pseudocapacitance. Pores with diameters <2 nm are accessible only to de-solvated ions and enable faradaic reactions [66].

Carbide-derived Carbon (CDC)

Carbide-derived carbon (CDC), also known as tunable nanoporous carbon, is the common term for carbon materials derived from carbide precursors, such as binary (e.g., SiC, TiC), or ternary carbides, also known as max phases (e.g., Ti_2AlC, Ti_3SiC_2) [67-71]. CDCs have also been derived from polymer-derived ceramics such as Si-O-C or Ti-C, and carbonitrides, such as Si-N-C [72-74]. CDCs can occur in various structures, ranging from amorphous to crystalline carbon, from sp^2- to sp^3-bonded, and from highly porous to fully dense. Carbide-derived carbons are used as an active material in electrodes for electric double-layer capacitors which have become commonly known as supercapacitors or ultracapacitors. This is because of their good electrical conductivity combined with high surface area [75], large micropore volume [76] and pore size control [77] that enable them to match the porosity metrics of the porous carbon electrode to a certain electrolyte [78].

Onion-like carbons

Onion-like carbons are 0-dimensional carbon nanomaterials yielding a non-porous but highly conductive carbon network. They provide a SSA of up to 600 $m^2 g^{-1}$ which is fully accessible for ions. The combination of high conductivity and ion accessibility yield a high specific power. However, due to the small SSA the specific capacitance is limited to approximately 30 F g^{-1} [79].

Carbon nanotubes

Carbon nanotubes (CNTs) are expected to also be attractive for capacitor electrode materials. Their important and promising characteristics as capacitor electrode materials include not only on their large area of exposed surface and different storage spaces for electrolyte ions, but also

1 The content has been taken from Wikipedia and [80]

their high electrical conductivity. Comparison on conducting paths for electron and electrolyte ion is in an aligned carbon nanotubes and granular activated carbon.

Irreversible electrochemical reactions, such as electrolyte decomposition, easily occur at a high potential, which prevent the use of the capacitor at high voltage. On such an ideal surface of CNTs, therefore, a large capacitance of EDL is expected to be accompanied by a wide potential window. However, most of the CNTs are known to be bundled with each other due to the van der Waals force, where only the outermost tubes in a bundle are exposed to the electrolyte and so-called bundle spaces among tubes are difficult to use for the formation of EDL. Consequently, the debundling of most of the CNTs is required in order to make all the surfaces of the tubes available for EDL formation. The inner surface of nanotubes is also useful for the access of electrolyte ions if suitable openings are formed. An interlayer space in the wall of multi-walled nanotubes can be intercalated by an electrolyte ion such as Li +. Therefore, the intercalation might be possible also as a faradaic reaction to give a pseudo-capacitance. However, it must be pointed out that excess enlargement of the interlayer spaces by intercalation will cause some degradation of the electrode which shortens the cycle life of the capacitor. In Fig. 3, the conducting paths for electrolyte ions and electrons in the aligned CNTs are schematically compared with activated carbon (AC) [80].

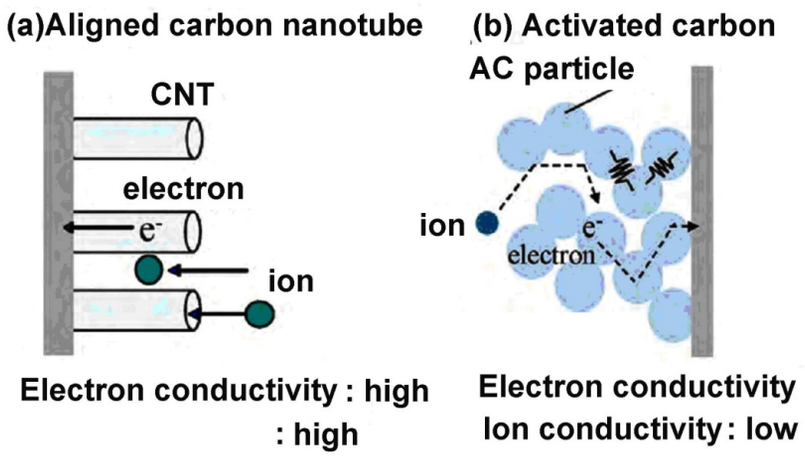

[Reprinted from [80] Inagaki M, Konno H, Tanaike O. Carbon materials for electrochemical capacitors. Journal of Power Sources. 2010, 195, 7880–7903, Copyright (2010), with permission from Elsevier].

Figure 3. Comparison of conducting paths for electron and electrolyte ion in an aligned carbon nanotubes and granular activated carbon.

Graphene

Overview of the properties of graphene

Graphene is a two-dimensional material consisting of a single layer of carbon atoms arranged in a honeycomb. It has been the subject of considerable research activities owing to its unusual and intriguing mechanical, thermal, electrical and optical properties [81–85]. Generally, a material's electrical and optical properties are closely related to its size and dimensions. This

is particularly reflected in the dimension control of graphene, both vertically and laterally [86] (figure 4).

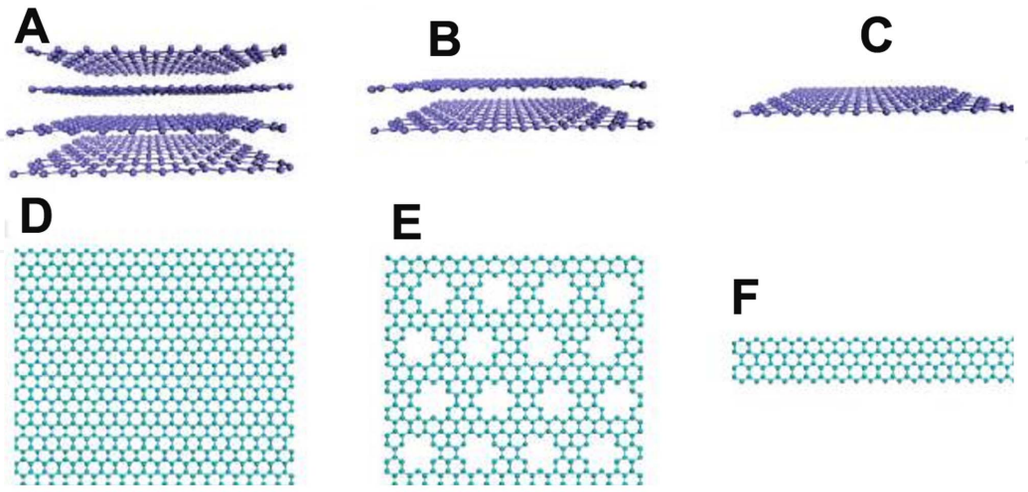

[Reprinted from [86] Sun, D. K. James, J.M. Tour, Graphene Chemistry: Synthesis and Manipulation,| J. Phys. Chem. Lett. 2011, 2, 2425–2432., Copyright (2011), with permission from ACS].

Figure 4. Manipulation of the geometry of graphene. Vertical control of graphene from (A) few-layer graphene to (B) bilayer graphene to (C) monolayer graphene. Lateral control of graphene from (D) plane sheet to (E) graphene mesh to (F) graphene ribbons.

With the advent of atomically thin and flat layers of graphene, new designs for thin film energy storage devices with good performance have become possible [87].

2.3. Utilization of graphene for EDLCs

One graphene-based supercapacitor uses curved graphene sheets that do not stack face-to-face, forming mesopores that are accessible to and wettable by environmentally friendly ionic electrolytes at voltages up to 4 V. They have a specific energy density of 85.6 Wh/kg (308 kJ/kg) at room temperature equalling that of a conventional nickel metal hydride battery, but with a power density 100-1000 times greater [88, 89].

The two-dimensional structure of graphene improves its charging and discharging. Charge carriers in vertically oriented sheets can quickly migrate into or out of the deeper structures of the electrode, thus increasing currents. Such capacitors may be suitable for 100/120 Hz filter applications, which are unreachable by supercapacitors using other carbons [90].

2.4. Graphene-based electrodes for EDLCs

The first utilization of graphene as an active material for an EDLC electrode was reported by Vivekchand et al. in early 2008 [91]. In order to develop energy storage devices with high power and energy densities, electrodes should hold well-defined pathways for efficient ionic and electronic transport. Choi et al. [92] demonstrate high-performance supercapacitors by building a three-dimensional (3D) macroporous structure that consists of chemically modified

http://dx.doi.org/10.5772/59201

graphene (CMG). These 3D macroporous electrodes, namely, embossed-CMG (e-CMG) films, were fabricated by using polystyrene colloidal particles as a sacrificial template. Furthermore, for a further capacitance boost, a thin layer of MnO_2 was additionally deposited onto e-CMG. The porous graphene structure with a large surface area facilitates fast ionic transport within the electrode while preserving decent electronic conductivity and thus endows MnO_2/e-CMG composite electrodes with excellent electrochemical properties, such as a specific capacitance of 389 F/g at 1 A/g and 97.7% capacitance retention upon a current increase to 35 A/g. Moreover, when the MnO_2/e-CMG composite electrode was asymmetrically assembled with an e-CMG electrode, the assembled full cell shows remarkable cell performance: an energy density of 44 Wh/kg, a power density of 25 kW/kg and an excellent cycle life.

Yoo et al. [93] reported an "in-plane" fabrication approach for ultrathin supercapacitors based on electrodes comprised of pristine graphene and multilayer reduced graphene oxide. The in-plane design is straightforward to implement and efficiently exploits the surface of each graphene layer for energy storage. The open architecture and the effect of graphene edges enable even the thinnest of devices, made from as-grown 1-2 graphene layers, to reach specific capacities up to 80 μFcm^{-2}, while much higher (394 μFcm^{-2}) specific capacities are observed in multilayer reduced graphene oxide electrodes. The performances of devices with pristine as well as thicker graphene-based structures are examined using a combination of experiments and model calculations. The demonstrated all solid-state supercapacitors provide a prototype for a broad range of thin-film-based energy storage devices. Table 1 shows a performance evaluation and comparison of the G and RMGO 2D "In-plane" supercapacitors.

		device properties[a]			electrode properties[b]				
							specific capacity		
mater	method	N	T (nm)	capacitance (μF)	mass (μg)	geometrical area (cm^2)	F g^{-1} [c]	μF cm^{-2} [d]	μF cm^{-2} [e]
G	CVD	1		3.333		0.1 × 0.835		80	80
RMGO	LBL	21[f]	10	35	0.283	0.085 × 2.1	247	394	19

[a] N = number of layers; T = thickness of the electrode. The capacitance values are reported for the best performance obtained using the CD curves with current density of 281 n Acm^{-2} for RMGO and 630 mAcm^{-2} for G. [b] Electrode capacitance converted from the device capacitance assuming asymmetrical capacitor. [c] Normalized by the electrode mass. [d] Normalized by one electrode's geometrical area. [e] Normalized by one electrode's interface area. [f] Calculated using the mass, the geometrical area, and the specific area of one side of graphene (1310 m^2 g -1).

[Reprinted from [93] Yoo J J, Balakrishnan K, Huang J, Meunier V, Sumpter B G, Srivastava A, Conway M, Mohana Reddy AL, Yu J, Vajtai R, Ajayan PM. Ultrathin Planar Graphene Supercapacitors, Nano Lett. 2011, 11, 1423–1427, Copyright (2011), with permission from ACS].

Table 1. Performance Evaluation and Comparison of the G and RMGO 2D "In-Plane" Supercapacitors

Ruoff group [94] has pioneered a new carbon material that we call chemically modified graphene (CMG). CMG materials are made from one-atom thick sheets of carbon, functionalized as needed, and here they demonstrate their performance in an ultracapacitor cell. Specific capacitances of 135 and 99 F/g in aqueous and organic electrolytes, respectively, have been measured. In addition, high electrical conductivity gives these materials consistently good

performance over a wide range of voltage scan rates. These encouraging results illustrate the exciting potential for high performance, electrical energy storage devices based on this new class of carbon material. Figure 4 shows a SEM image of a CMG particle surface, TEM image showing individual graphene sheets extending from the CMG particle surface, low and high (inset) magnification SEM images of CMG particle electrode surfaces, and the schematic of a test cell assembly. Figure 5d also shows a schematic of the two-electrode ultracapacitor test cell and fixture assembly. CMG-based ultracapacitor cells were tested with three different electrolytes commonly used in commercial EDLCs.

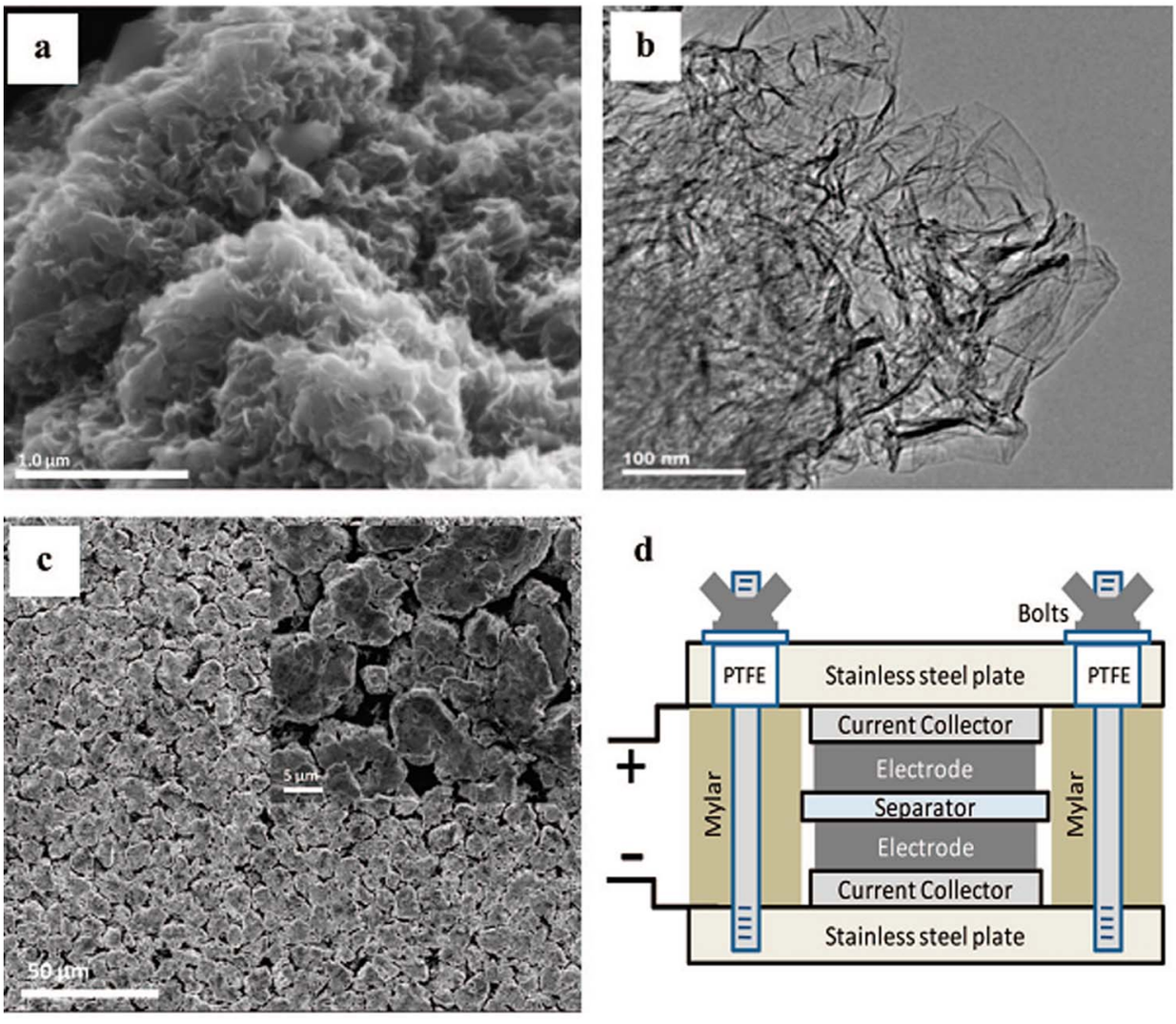

[Reprinted from [94] Stoller M D, Park S, Zhu Y, An J, Ruoff R S, Graphene-Based Ultracapacitors. Nano Lett.,2008; 8, 3498-3502, Copyright (2008), with permission from ACS]

Figure 5. (a) SEM image of CMG particle surface, (b) TEM image showing individual graphene sheets extending from CMG particle surface, (c) low and high (inset) magnification SEM images of CMG particle electrode surface, and (d) schematic of a test cell assembly.

A supercapacitor with graphene-based electrodes was found to exhibit a specific energy density of 85.6 Wh/kg at room temperature and 136 Wh/kg at 80 °C (all based on the total electrode weight), measured at a current density of 1 A/g by Liu et al. [95]. These energy density values are comparable to those of the Ni metal hydride battery, but the supercapacitor can be charged or discharged in seconds or minutes. The key to success was the ability to make full utilization of the highest intrinsic surface capacitance and the specific surface area of single-layer graphene by preparing curved graphene sheets that will not restack face-to-face. The curved morphology enables the formation of mesopores accessible to and wettable by environmentally benign ionic liquids capable of operating at a voltage >4V. Highly corrugated graphene sheets (HCGS) were prepared by a rapid, low-cost and scalable approach through the thermal reduction of graphite oxide at 900 °C followed by rapid cooling using liquid nitrogen by Yan et al. [96]. The wrinkling of the graphene sheets can significantly prevent them from agglomerating and restacking against one another face to face and thus increase the electrolyte-accessible surface area. The maximum specific capacitance of 349 F g^{-1} at 2mV s^{-1} is obtained for the HCGS electrode in a 6 M KOH aqueous solution. Additionally, the electrode shows excellent electrochemical stability along with an approximately 8.0% increase of the initial specific capacitance after 5000 cycle tests. These features make the present HCGS material a quite promising alternative for the next generation of high-performance supercapacitors.

2.5. The electrolytes

The performance of a supercapacitor is not only dependent on the electrode materials, but is also strongly affected by the electrolytes employed. A high cell operating voltage provides both high energy density and power density, but is limited by the stability of the electrolyte in the applied potential. The most recent supercapacitors available in the market use electrolytes based on aprotic solvents, typically acetonitrile or carbonate-based solvents (i.e., propylene carbonate) [97].

2.5.1. Electrolyte solution[2]

Most of the commercial EDLCs use non-aqueous electrolyte solutions to achieve a high terminal voltage, V, because the capacitor energy, E, and the maximum power, P_{max}, are given by:

$$E = CV^2/2 \text{ and } Pmax = V^2/4R$$

where C is the cell capacitance in F and R is the internal resistance in Ω. The EDLCs that use non-aqueous electrolyte solutions dominate the market for capacitors focusing on energy storage, but those that use aqueous electrolyte solutions are also marketed. Aqueous solutions are potentially beneficial to large installations for the storage of surplus power and unsteady

2 *The content has been taken from [80]*

electricity generated by natural energy resources, because of their low cost, high safety, long lifetime and low internal resistance. Representative electrolytes and solvents (with abbreviations) are listed in Table 1, where some of their properties are also indicated [80, 98].

In EDLCs, the sizes of the cation and anion of the electrolyte are important factors in relation to the surface area, effective for the adsorption of the ions, of the electrode carbons. In the case of non-aqueous electrolyte solutions numerous combinations of electrolytes, both organic and inorganic, with solvents are possible. The solvent itself also affects the capacitance [99,100] and one combination is not always optimum for all carbon materials. When the electrolytes containing lithium ions were used in EDLC, it was shown that the intercalation of Li^+ ions occurred together with its adsorption onto the surface of the carbon electrode [101], which is also used in hybrid capacitors, as will be described below [80]. Table 2 shows electrolytes and solvents that are often used.

Electrolytes	Ion size (nm)	
	Cation	Anion
Organic electrolytes		
$(C_2H_5)_4N{\cdot}BF_4$ ($TEA^+BF_4^-$)	0.686	0.458
$(C_2H_5)_3(CH_3)N{\cdot}BF_4$ ($TEMA^+BF_4^-$)	0.654	0.458
$(C_2H_5)_4P{\cdot}BF_4$ ($TEP^+BF_4^-$)		0.458
$(C_4H_9)_4N{\cdot}BF_4$ ($TBA^+BF_4^-$)	0.830	0.458
$(C_6H_{13})_4N{\cdot}BF_4$ ($THA^+BF_4^-$)	0.96	0.458
$(C_2H_5)_4N{\cdot}CF_3SO_3$	0.686	0.540
$(C_2H_5)_4N{\cdot}(CF_3SO_2)_2N$ (TEA^+TFSI^-)	0.68	0.650
Inorganic electrolytes		
H_2SO_4		0.533
KOH	0.26[a]	
Na_2SO_4	0.36[a]	0.533
NaCl	0.36[a]	
$Li{\cdot}PF_6$	0.152[b]	0.508
$Li{\cdot}ClO_4$	0.152[b]	0.474

Solvents	Melting point (°C)	Viscosity ($Pa\,s^{-1}$)	Dielectric constant, ε
Acetonitrile (AN)	−43.8	0.369	36.64
γ-Butyrolactone (GBL)	−43.3	1.72	39.0
Dimethyl ketone (DMK)	−94.8	0.306	21.01
Propylene carbonate (PC)	−48.8	2.513	66.14
Water			

[a] Stokes diameter of hydrated ions.

[b] The diameter in PC, depending strongly on the solvent used.

[Reprinted from [80] Inagaki M, Konno H, Tanaike O. Carbon materials for electrochemical capacitors. Journal of Power Sources. 2010, 195, 7880–7903, Copyright (2010), with permission from Elsevier].

Table 2. Electrolytes and solvents that are often used.

Ionic liquid (IL)-based electrolytes containing molecular solvents were also shown to be attractive for extreme temperature applications in electric double-layer capacitors (EDLCs).

2.5.1.1. Supercapacitors: Ionic liquid electrolytes[3]

Certain unique properties of these environmentally friendly ionic liquids, including high ionic conductivity (up to 10^{-2} Scm^{-1}), large liquid phase range (−100–400 °C), wide electrochemical window (4–6V), non-volatility, non-flammability, and non-toxicity, have made them an excellent electrolyte for electrochemical energy. The ionic liquids mainly studied for supercapacitor application are imidazolium, pyrrolidinium and asymmetric aliphatic quaternary ammonium salts of anions such as tetrafluoroborate (BF_4), trifluoromethanesulfonate (Tf), bis(trifluoromethanesulfonyl)imide (TFSI) (bis(fluorosulfonyl)imide (FSI), and hexafluorophosphate (PF_6), and all feature an ESW wider than that of the conventional organic electrolytes at RT. The ESW is defined as the potential range limited by the cathodic and anodic stability potentials evaluated on glassy carbon or platinum smooth electrodes. Figure 6 shows conductivity and ESW data at RT of some ionic liquids based on 1-ethyl-3-methylimidazolium (EMI), 1-butyl-3-methylimidazolium (BMIM), N-diethyl- N-methyl(2-methoxyethyl)ammonium (DEME), N-butyl-N-methyl-pyrrolidinium (PYR_{14}), N-methyl- N-propyl-pyrrolidinium (PYR_{13}), and N-methoxyethyl- N-methylpyrrolidinium cations with different anions [102].

The interface models developed for high-temperature molten salts are not completely appropriate for ionic liquids, mainly because of the weaker cation–anion interactions in ionic liquids than in molten salts. On the contrary, the absence of solvents in ionic liquids implies that the double layer cannot be described by the Helmholtz model developed for conventional concentrated electrolyte solutions, as depicted in Figure 7. In such solutions, the solvent molecules in the inner Helmholtz plane (IHP) separate electrode surface charges and electrolyte counter ions located in the outer Helmholtz plane (OHP) by a distance l, so that the solvent molecular size, rather than ion size, and solvent dielectric constant (e) significantly affect electrode capacitance (C_e), which is given by:

$$C_e = k^o \varepsilon A/l \tag{2}$$

where κ^o= 8.85×10-12 Fm^{-1} and A is the electrode surface area. In the case of solvent-free ILs, the electrified electrode surface comes up against the ionic liquid counter ions located in the IHP. Thus, the relation between C_e and A depends on the ionic liquid ion chemistry and structure at the electrode–IL interface. The size, orientation under electric field and polarizability of ionic liquids directly affect thickness, the dielectric constant of the double layer, and the capacitive response of the electrodes [102].

2.5.1.2. Ionic liquids as electrolyte for activated carbon, carbon nanotubes and associated composite supercapacitors

Before protic ionic liquid as an electrolyte for high-density electrochemical double-layer capacitors with activated carbon electrode material prior can be implemented for grid-scale applications of the energy storage devices, there remain several key issues to address including

3 The content has been taken from [102]

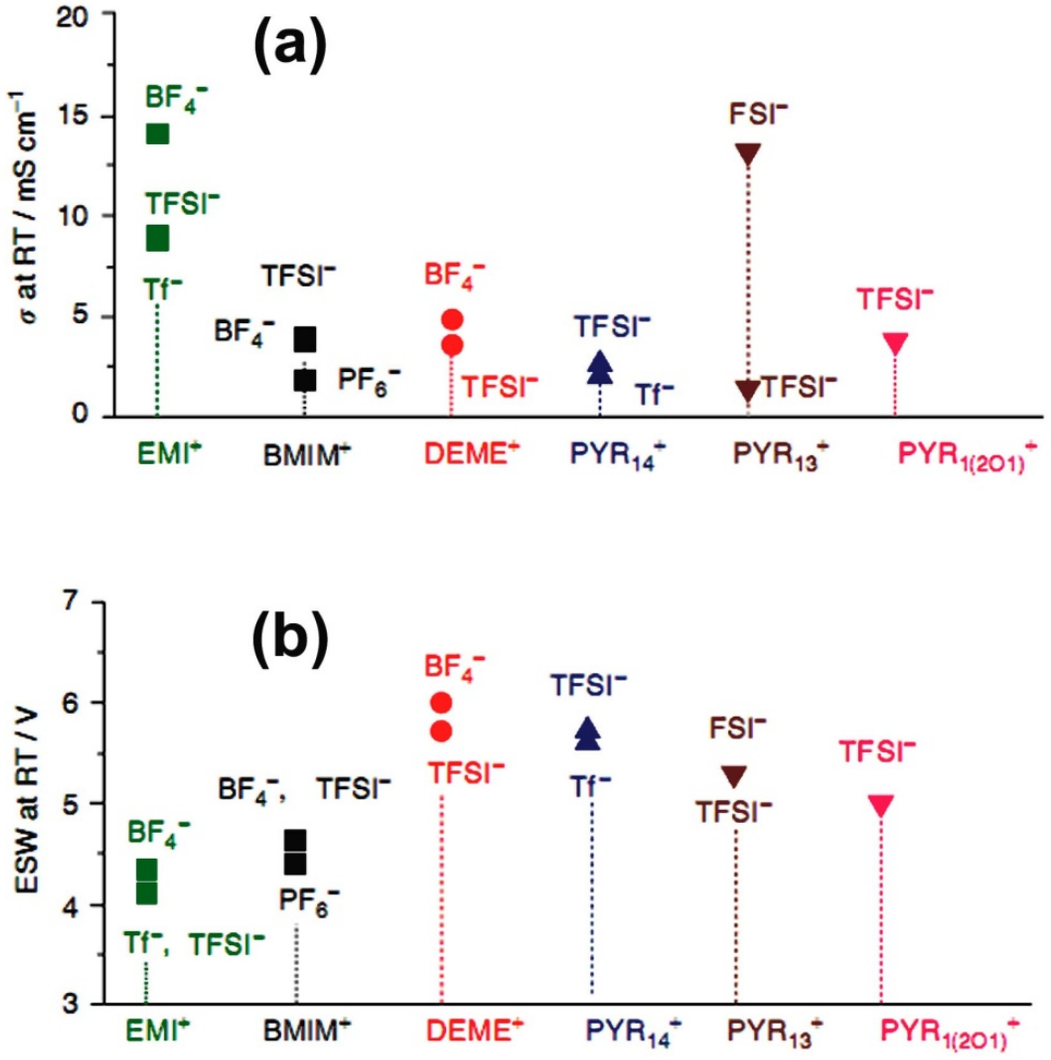

[Reprinted from [102] Mastragostino M, Soavi F. Electrochemical Capacitors: Ionic Liquid Electrolytes, Reference Module in Chemistry, Molecular Sciences and Chemical Engineering, Elsevier, 2009, Pages 649–657, Copyright (2009), with permission from Elsevier].

Figure 6. (a) Conductivity (σ) and (b) electrochemical stability window (ESW) data at room temperature of ILs based on 1-ethyl-3-methylimidazolium (EMI), 1-butyl-3-methylimidazolium (BMIM), N-diethyl-N-methyl(2-methoxyethyl)ammonium (DEME), N-butyl-N-methyl-pyrrolidinium (PYR_{14}), N-methyl-N-propyl-pyrrolidinium (PYR_{13}), and N-methoxyethyl-N-methylpyrrolidinium cations with different anions.

the development of low-cost, high-performance materials and electrolytes which are environmentally friendly and compatible with low-temperature and large-scale processing. Anouti et al. [103] reported the preparation, characterization and comparative application of two protic ionic liquids namely, diisoprpylethylammonium methanesulfonate, [DIPEA][$MeSO_3$], and pyrrolidinium methanesulfonate, [Pyrr][$MeSO_3$], in a mixture with water as an electrolyte for supercapacitor applications. Different electrochemical measurements like cyclic voltammetry (CV), electrochemical impedance spectroscopy (EIS), and galvanostatic charge–discharge were conducted to study the performance of these aqueous solutions as supercapacitors with an activated carbon electrode.

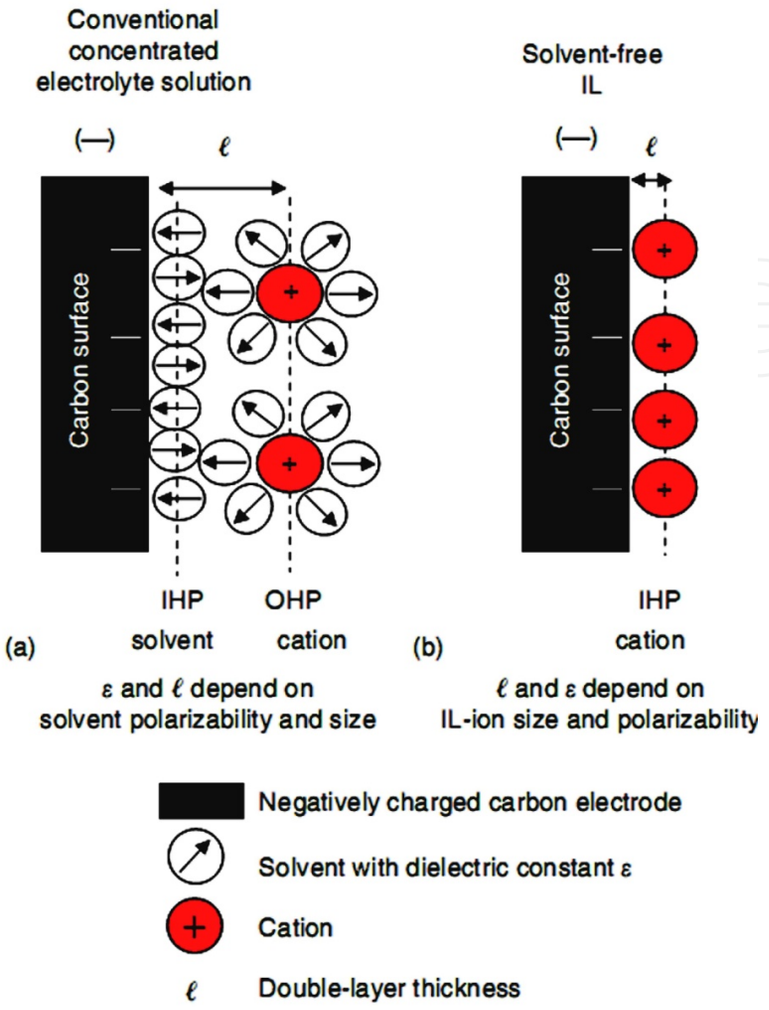

[Reprinted from [102] Mastragostino M, Soavi F. Electrochemical Capacitors: Ionic Liquid Electrolytes, Reference Module in Chemistry, Molecular Sciences and Chemical Engineering, Elsevier, 2009, Pages 649–657, Copyright (2009), with permission from Elsevier].

Figure 7. Schematic representation of the double layer at the negatively charged carbon electrode–electrolyte interface in (a) conventional electrolyte solution and (b) solvent-free ionic liquid electrolyte.

From this work, good specific capacitances of up to 102 F g^{-1} have been observed even at high-rate cyclability, as well as an increase of the specific power close to 13.9 kW kg^{-1} at a high current density of 15 A g^{-1}. Fig. 7 shows galvanostatic charge/discharge and capacitance as a function of current density for DIPEA methanesulfonate in water (w = 0.707) and pyrrolidinium methanesulfonate in water (w = 0.557). Figure 8 shows galvanostatic charge/discharge and capacitance as a function of the current density for DIPEA of methanesulfonate in water and pyrrolidinium methanesulfonate in water.

Balducci et al. [104] present results on the electrochemical and cycling characterizations of a supercapacitor cell using a microporous activated carbon as the active material and N-butyl-N-methylpyrrolidinium bis(trifluoromethanesulfonyl)imide (PYR14TFSI) ionic liquid as the electrolyte. The microporous activated carbon exhibited a specific capacitance of 60 F g^{-1}

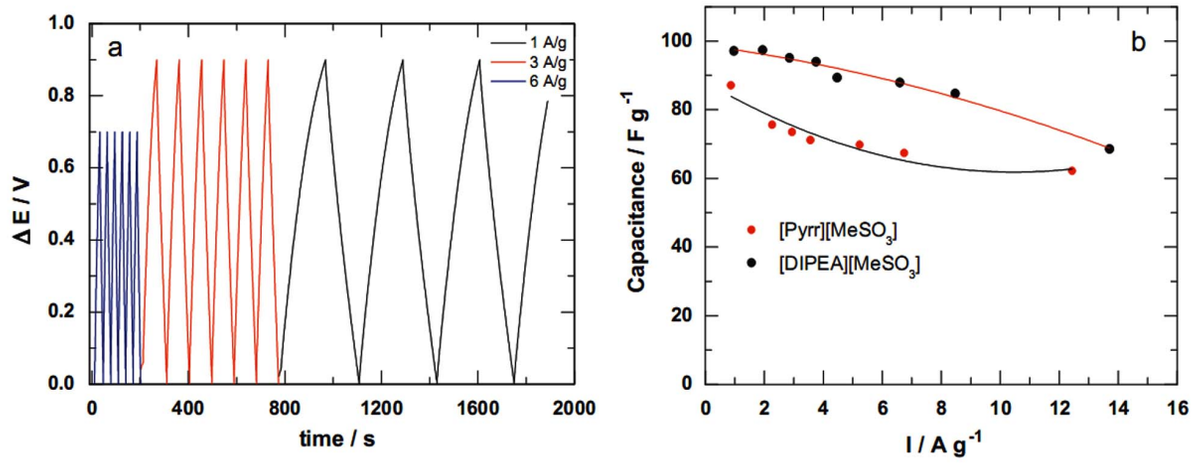

[Reprinted from [103] Anouti M, Couadou E, Timperman L, Galiano H. Protic ionic liquid as electrolyte for high-densities electrochemical double-layer capacitors with activated carbon electrode material. Electrochimica Acta. 2012, 64, 110–117, Copyright (2012), with permission from Elsevier].

Figure 8. Galvanostatic charge/discharge (a) and capacitance (b) as a function of current density for DIPEA methanesulfonate in water (w = 0.707) and pyrrolidinium methanesulfonate in water (w = 0.557).

measured from the three-electrode cyclic voltammetry experiments at a 20mVs^{-1} scan rate, with a maximum operating potential range of 4.5V at 60 ºC. A coin cell assembled with this microporous activated carbon and PYR$_{14}$TFSI as the electrolyte were cycled for 40,000 cycles without any change in cell resistance (9cm2), at a voltage up to 3.5 V at 60 ºC, demonstrating a high cycling stability as well as a high stable specific capacitance in this ionic liquid electrolyte. These high performances now make this type of supercapacitor suitable for high temperature applications (≥60 ºC). Protic ionic liquids (PILs) have been proposed as novel electrolytes for supercapacitors by Brandta et al. [105]. Nevertheless, so far the long term cycling stability of PIL-based supercapacitors has never been investigated in detail. Since high cycling stability is essential for such devices, a study about this aspect therefore appears to be of importance for understanding the advantages and the limits of PIL-based systems. In this work we showed that using protic ionic liquids as electrolytes, it is possible to implement electrochemical double-layer capacitors (EDLCs) with an operative voltage as high as 2.4 V, able to feature good cycling stability in a broad range of temperatures. Moreover, we also showed that the pseudo-capacitive behaviour of activated carbon (ACs) in these electrolytes strongly depends on the water content and on the surface groups present on the ACs. When protic ionic liquids with a lower content of water were used in combination with AC containing few surface groups, PIL-based supercapacitors exhibit specific capacitance comparable to classical organic electrolytes without any evident pseudo-capacitive contribution.

Figure 9 shows the chemical structures of the protic ionic liquids (a) triethylammonium bis(tetrafluoromethylsulfonyl)imide ($Et_3NHTFSI$), (b) trimethylammonium bis(tetrafluoromethylsulfonyl)imide ($Me_3NHTFSI$) and (c) pyrrolidinium nitrate ($PYRNO_3$).

Table 3 shows ionic conductivities, electrochemical stability windows (ESWs) and the protic ionic liquids' mole fractions of the used electrolytes containing protic ionic liquids at 20 °C.

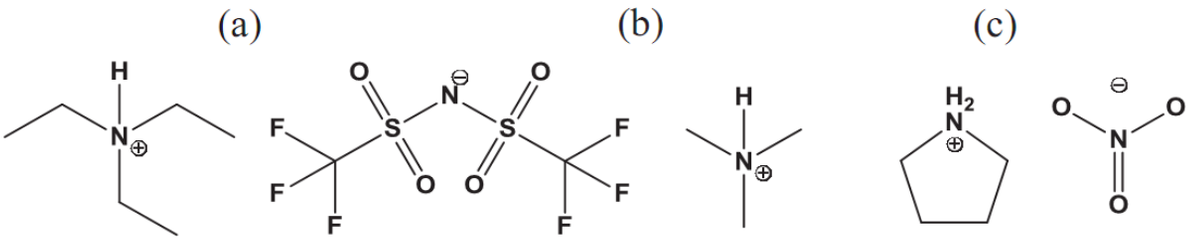

[Reprinted from [105] Brandt A, Pires J, Anouti M, Balducci A. An investigation about the cycling stability of supercapacitors containing protic ionic liquids as electrolyte components. Electrochimica Acta 2013,108, 226– 231, Copyright (2013), with permission from Elsevier].

Figure 9. Chemical structures of the protic ionic liquids (a) triethylammonium bis(tetrafluoromethylsulfonyl)imide ($Et_3NHTFSI$), (b) trimethylammonium bis(tetrafluoromethylsulfonyl)imide ($Me_3NHTFSI$) and (c) pyrrolidinium nitrate ($PYRNO_3$).

Electrolyte	Conductivity ($mS\ cm^{-1}$)	ESW (V)	PIL mole fraction (%)
$Et_3NHTFSI$	4	3.8	100
PC-$Me_3NHTFSI$	13.6	3.9	23
PC-$PYRNO_3$	14.0	2.6	42

[Reprinted from [105] Brandt A, Pires J, Anouti M, Balducci A. An investigation about the cycling stability of supercapacitors containing protic ionic liquids as electrolyte components. Electrochimica Acta 2013,108, 226– 231, Copyright (2013), with permission from Elsevier].

Table 3. Ionic conductivities, electrochemical stability windows (ESWs) and protic ionic liquids' mole fractions of the used electrolytes containing protic ionic liquids at 20 °C.

Coadou et al. [106] report a comparative study on the performances of two bis[(trifluoromethyl)sulfonyl]imide-based protic (PIL) and aprotic (AIL) ionic liquids, namely, trimethylammonium bis[(trifluoromethyl)sulfonyl]imide ($[HN_{111}][TFSI]$, PIL) and trimethyl-sulfonium bis[(trifluoromethyl)sulfonyl]imide ($[S_{111}][TFSI]$, aprotic ionic liquids), as mixtures with three molecular solvents: gamma butyrolactone (γ-BL), propylene carbonate (PC) and acetonitrile (ACN) as electrolytes for supercapacitor applications. After an analysis of their transport properties as a function of temperature, cyclic voltammetry (CV), electrochemical impedance spectroscopy (EIS), and galvanostatic charge–discharge, measurements were conducted at 25 and −30 °C to investigate the performance of these mixtures as electrolytes for supercapacitors using activated carbon as the electrode material. Surprisingly, for each solvent investigated, no significant differences were observed between the electrolytes based on the protic ionic liquids and aprotic ionic liquids in their electrochemical performance due to the presence or the absence of the labile proton. Furthermore, good specific capacitances were observed in the case of γ-BL-based electrolytes even at low temperatures. Capacitances of up to 131 and 80 F

g^{-1} are observed for the case of the $[S_{111}][TFSI]$ + γ-BL mixture at 25 and −30 °C, respectively. This latter result is very promising particularly for the formulation of new environmentally friendly electrolytes within energy storage systems even at low temperatures. Lu reported [107] a new class of nanocomposite electrodes for the development of high-performance supercapacitors with environmentally friendly ionic liquid electrolytes. Having high-surface-area activated carbons, carbon nanotubes, and ionic liquids as integrated constituent components, the resultant composites show significantly improved charge storage and delivery capabilities. In an ionic liquid electrolyte, the composites possess a superior capacitance (188 F/g) over a pure carbon nanotube electrode (20 F/g) and a conventional activated carbon electrode (90 F/g). On the basis of these nanocomposite electrodes and an ionic liquid electrolyte, we have further developed prototype supercapacitors with a high cell voltage (4 V), and superior energy and power densities (50 Wh/kg and 22 kW/kg, respectively, in terms of the mass of the active electrode material). The nanocomposite supercapacitors developed in this study clearly outperform the current supercapacitor technology, providing a new approach in fabricating advanced supercapacitors with a high-performance, inherently safe operation and long lifetime. Zhao et al. [108] reported the synthesis of novel nanocomposite electrodes based on MnO_2 nanosheets, Pt, Au, or Pd nanoparticles (NPs), exfoliated carbon nanotubes (CNTs), and Ni foam (NF) substrates. The MnO_2Pd–CNT–NF electrode in 1-butyl-3-methyl-imidazolium hexafluorophosphate (BMIM-PF_6)/N, N-dimethylformamide (DMF) electrolyte exhibits a high specific capacitance of 559.1 F/g based on MnO_2 with a wide potential window (2.1 V). To the best of our knowledge, this is one of the highest capacitance for MnO_2 in ionic liquid (IL) electrolytes ever reported. The IL hybrid supercapacitors are assembled using MnO_2–Pd–CNTs–NF positive electrodes, activated carbon (AC) negative electrodes, and BMIM-PF_6/DMF electrolyte displaying a high operating voltage (3 V), high energy density (78.4Wh/kg) and high power density (12.7 kW/kg). The superior performances of the MnO_2 IL hybrid supercapacitors suggest their potential application for the future generation of electrochemical power sources. The ionic liquids (ILs) *N*-butyl-*N*-methyl-pyrrolidinium trifluoromethanesulfonate ($PYR_{14}Tf$) and *N*-methyl-*N*-propyl-pyrrolidinium bis(fluorosulfonyl)imide ($PYR_{13}FSI$) are investigated as electropolymerization media for poly(3-methylthiophene) (pMeT) in view of their use in carbon/IL/pMeT hybrid supercapacitors by Biso et al. [109]. Data on the viscosity, solvent polarity, conductivity and electrochemical stability of $PYR_{14}Tf$ and $PYR_{13}FSI$ as well as the effect of their properties on the electropolymerization and electrochemical performance of pMeT, which features >200 Fg^{-1} at 60°C when prepared and tested in such ionic liquids, are reported and discussed; the results of the electrochemical characterization in N-butyl-N-methyl-pyrrolidiniumbis(trifluoromethanesulfonyl)imide of the so-obtained pMeT are also given, for comparison.

2.5.1.3. Ionic liquids as electrolyte for graphene, graphene oxide and associated composite supercapacitors

The activation behaviour and achievable specific capacitance of intercalation-like carbon materials, such as partially reduced graphite oxide (GOpr), employing pure and diluted ionic liquids were investigated by Hantel et al. [110]. The electrochemical activation of two different GOprs with interlayer distances of 3.9 and 4.4 A° and a graphite was studied with the ionic

liquid 1-ethyl-3-methyl-imidazolium tetrafluoroborate ($EMIMBF_4$). Furthermore, the effect of the organic solvent acetonitrile (AN) on the activation was tested by a stepwise dilution of the ionic liquid. It is shown that a rudimentary electrochemical activation of GOpr is possible with $EMIMBF_4$. However, the resulting specific capacitance was below 100 F g^{-1} indicating an incomplete activation reaction. By the stepwise dilution of $EMIMBF_4$ with AN, the specific capacitance was increased up to approximately 180 F $g^{-1.}$ Therefore, it seems that the electrochemical activation of intercalation-like carbon materials was based on both a reaction with the ions as well as with the employed solvent. Moreover, this experimental study indicates that an increased molarity of organic electrolytes has no influence on the maximum achievable specific capacitance. Figure 8 visualizes the specific capacitances for the different molarities of $EMIMBF_4$/AN, which are calculated from galvanostatic discharge measurements at 0.1 Ag^{-1}. If a decreased molarity and thus a lack of ions results in a decreasing specific capacitance, they double and reach a stable value for molarities smaller than 5.2 M $EMIMBF_4$/AN. For molarities between 0.9 and 5.2 M $EMIMBF_4$/AN, the specific capacitances of GOpr44 and GOpr39 are similar with approximately 180 ± 10 F g^{-1}. Therefore, even an ion concentration of 0.9 M seems to be enough to reach the maximum achievable specific capacitance. A summary of positive (red) and negative (blue) polarization cycles after electrochemical activation for a changing concentration of EMIMBF4/AN for GOpr44 is shown in figure 10.

Tamilarasan et al. [111] reported the fabrication of a mechanically stable, flexible graphene-based all-solid-state supercapacitor with ionic liquid incorporated polyacrylonitrile (PAN/[BMIM][TFSI]) electrolyte for electric vehicles (EVs). The PAN/[BMIM][TFSI] electrolyte shows high ionic conductivity (2.42 mS/cm at 28 °C) with high thermal stability. The solid-like layered phase of ionic liquid is observed on the surface of the pores of the PAN membrane along with a liquid phase which made it possible to hold 400 wt% of the mobile phase. This phase formation is facilitated by the ionic interaction of C≡N moieties with the electrolyte ions. A supercapacitor device, comprised of PAN/[BMIM][TFSI] electrolyte and graphene as the electrode, is fabricated and its performance is demonstrated. Several parameters of the device, such as energy storage and discharge capacity, internal power dissipation, operating temperature, safe operation and mechanical stability, meet the requirements of future EVs. In addition, a good cyclic stability is observed even after a drop of 1000 cycles of potential.

Figure. 10 shows the energy density and power density of 30.51 Wh/kg and 15.34 kW/kg, respectively, at the specific current of 10 A/g corresponding to the Cs of 98 F/g, in terms of the mass of the total electrode material. The Ragone plot drops faster with the power due to the fast voltage decay during discharge at high power. The maximum energy storage capacity (Emax) and the maximum reduced graphene oxide (RGO) was prepared with HBr as a reducing reagent. RGO-based supercapacitors in two-electrode systems have been fabricated in ionic liquid electrolytes of 1-butyl-3-methylimidazolium hexafluorophosphate ($BMIPF_6$) and 1-butyl-3-methylimidazolium tetrafluoroborate ($BMIBF_4$), respectively by Chen et al. [112].

RGO in $BMIBF_4$ shows a higher capacitance of 74 F g^{-1} at 10 mV s^{-1}, while RGO in $BMIPF_6$ merely exhibits 45 F g^{-1}. However, due to the wider potential window of 4 V for $BMIPF_6$, RGO in $BMIPF_6$ has higher energy and power densities. The highest power density of 27.8 $kWkg^{-1}$

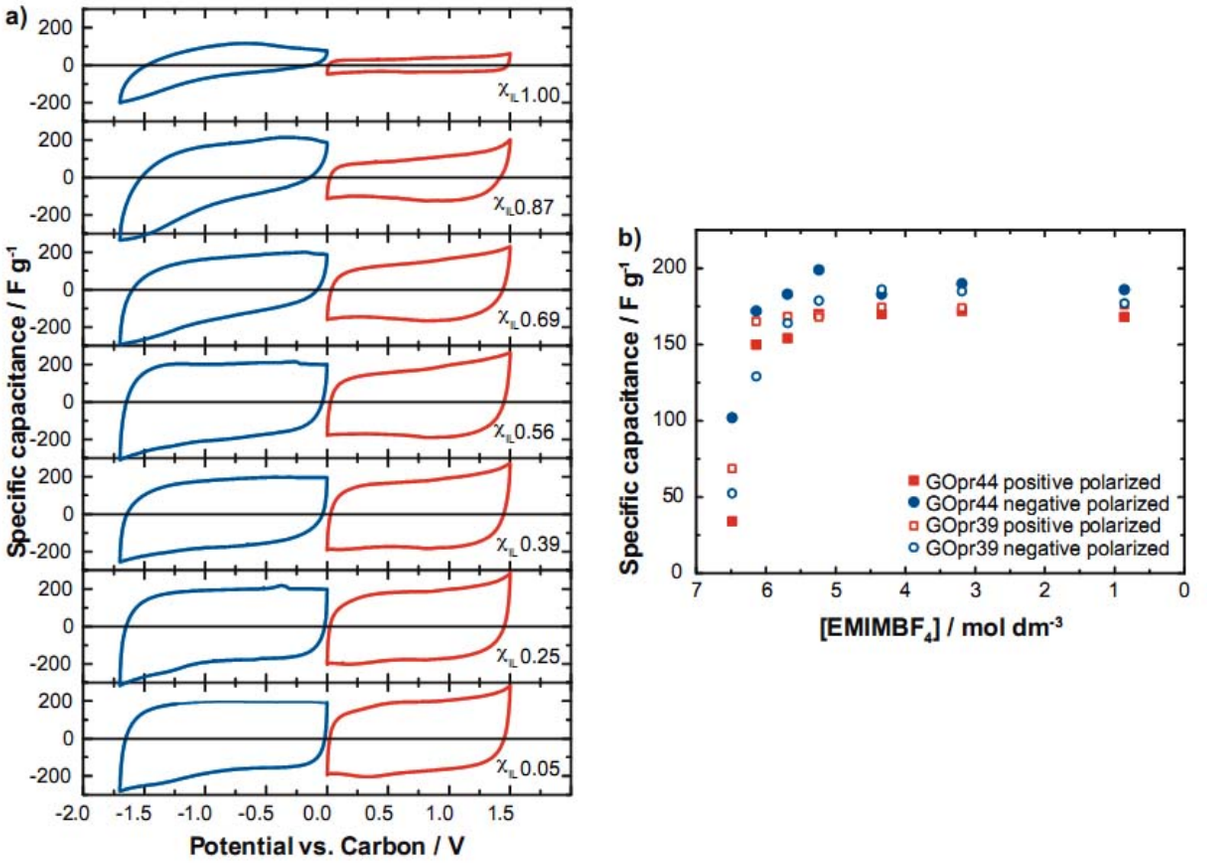

[Reprinted from [110] Birbilis N, Bouzek K, Bultel Y, Cuesta A, Ferapontova E, Hartl F, Hebert K, Jones D J, Komaba S, Kuhn A, Hantel M M, Płatek A, Kaspar T R, Nesper R, Wokaun A, Kötz R. Investigation of diluted ionic liquid 1-ethyl-3-methyl-imidazolium tetrafluoroborate electrolytes for intercalation-like electrodes use supercapacitors. Electrochimica Acta.2013; 110, 234–239, Copyright (2013), with permission from Elsevier].

Figure 10. (a) Summary of positive (red) and negative (blue) polarization cycles after electrochemical activation for a changing concentration of $EMIMBF_4$/AN for GOpr44. The CVs were all taken with a sweep rate of 1 mV s^{-1}. (b) Specific capacitance calculated from the galvanostatic discharge of a positive polarized (red squares) or negative polarized (blue circles) GOpr39 (open symbols) and GOpr44 (filled symbols), respectively at 0.1 Ag^{-1} as a function of the molarity of $EMIMBF_4$/AN. (For an interpretation of the references to colour in this figure legend, the reader is referred to the web version of this article.)

is obtained at 14 A g^{-1} and the maximum energy density of 18.9Wh kg^{-1} at 1Ag^{-1} for $BMIPF_6$. The exciting results suggest the potential application of RGO in $BMIPF_6$. High specific surface area (SSA ~2000 m^2/g) porous KOH-activated microwave exfoliated graphite oxide ('a-MEGO') electrodes have been tested in a eutectic mixture of ionic liquids (1:1 by weight or molar ratio N-methyl-N-propylpiperidinium bis(fluorosulfonyl)imide (PIP13-FSI) and N-butyl-N-methylpyrrolidinium bis(fluorosulfonyl)imide (PYR14-FSI)) as an electrolyte for supercapacitor applications by Tsai et al. [113].

By optimizing the carbon/electrolyte system, outstanding capacitive performance has been achieved with high capacitance (up to 180 F/g) and a wide electrochemical window (up to 3.5 V) over a wide temperature range from -50 °C to 80 °C. This is the first demonstration of a

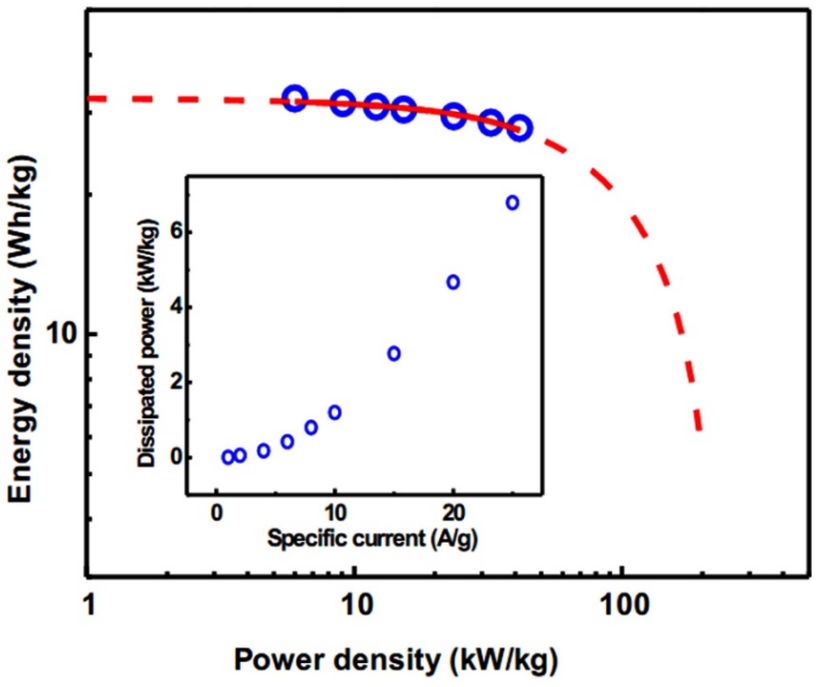

[Reprinted from [111] Tamilarasan P, Ramaprabhu S. Graphene-based all-solid-state supercapacitors with ionic liquid incorporated polyacrylonitrile electrolyte, Energy.2013; 51, 374-381, Copyright (2013), with permission from Elsevier].

Figure 11. Ragone plot of HEG e PAN/[BMIM][TFSI] supercapacitor. Inset: power dissipated in equivalent series resistance RESR (PESR) as a function of specific current.

carbon–ionic liquid system capable of delivering capacitance in excess of 100 F/g below room temperature. The excellent electrochemical response of the proposed couple shows that optimization of the carbon/electrolyte interface is of great importance for improving capacitive energy storage. Wei et al. studied [114] the application of different types of room temperature ionic liquids (RTILs) into flexible supercapacitors. Typical RTILs including 1-buthyl-3-methyl-imidazolium [BMIM][Cl], trioctylmethylam monium bis(trifluoromethylsulfonyl)imide [OMA][TFSI] and triethylsulfonium bis(trifluoromethylsulfonyl)imide ([SET_3][TFSI]) were studied. [SET_3][TFSI] shows the best result as an electrolyte in electrochemical double-layer (EDLC) supercapacitors, with a very high specific capacitance of 244 F/g at room temperature, overceiling the performance of conventional carbonate electrolytes such as dimethyl carbonate (DMC) with a more stable performance and much larger electrochemical window. Fig. 12 shows the cyclic voltammogram curves of the supercapacitors with electrolytes.

Chatterjee et al. [115] demonstrate the electrochemical stability of nanostructured silicon in corrosive aqueous, organic, and ionic liquid media enabled by conformal few-layered graphene heterogeneous interfaces. They demonstrate direct gas-phase few-layered graphene passivation (d = 0.35 nm) at temperatures that preserve the structural integrity of the nanostructured silicon. This passivation technique is transferrable both to silicon nanoparticles (Si-NPs) as well as to electrochemically etched porous silicon (P-Si) materials. For Si-NPs, we find the graphene-passivated silicon to withstand physical corrosion in NaOH aqueous conditions

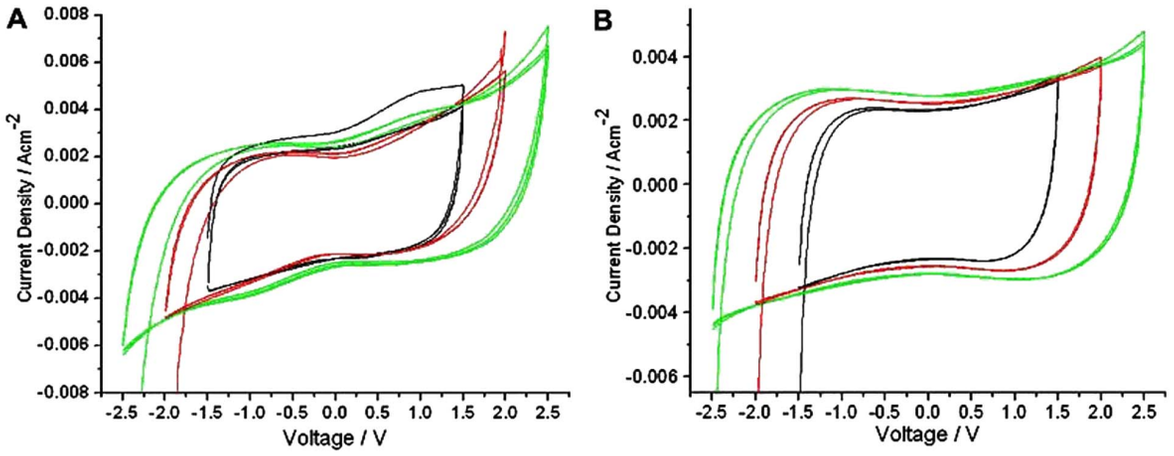

[Reproduced from [114] Wei D, Ng T W. Application of novel room temperature ionic liquids in flexible supercapacitors, Electrochemistry Communications.2009; 11, 1996–1999, Copyright (2009), with permission from Elsevier].

Figure 12. The cyclic voltammogram curves of the supercapacitors with electrolytes of (A) 5 wt% LiTFSI in DMC (B) 5 wt% LiTFSI in [SET3][TFSI]. Electrochemical window is in the range of -1.5 to 1.5 V, -2.0 to 2.0 V and -2.5 to 2.5 V with a scan rate of 50 mV/s

where unpassivated Si-NPs spontaneously dissolve. For P-Si, we demonstrate electrochemical stability with widely different electrolytes, including NaOH, enabling these materials for use in electrochemical supercapacitors. This leads us to develop high-power on-chip porous silicon supercapacitors capable of up to 10 Wh/kg and 65 kW/kg energy and power densities, respectively, and 5 Wh/kg energy density at 35 kW/kg—comparable to many of the best high-power carbon-based supercapacitors. As surface reactivity wholly dictates the utilization of nanoscale silicon in diverse applications across electronics, energy storage, biological systems, energy conversion, and sensing, we strongly suggest the direct formation of few-layered graphene on nanostructured silicon as a means to form heterogeneous on-chip interfaces that can maintain stability in even the most reactive of environments. Graphene nanosheets (GNS) were modified by 1-Butyl-3-methylimidazolium hexafluorophosphate, which is one of the ionic liquids (IL). Owing to the modification of graphene with ionic liquids, graphene can not only be structurally stabilized, but also showed the highest charge transfer that allows it to exhibit an enhanced electrochemical performance. Furthermore, a graphene aggregation by the intersheet van der Waals interaction can be prevented because ionic liquids act as an effective agent for the exfoliation of graphene sheets. The prepared composites showed the enhanced electrochemical performance such as high rate capability and excellent cycle performance [116]. Figure 13 shows a schematic representation of the preparation process of GNS/IL composites.

Figure 14 shows the cycle performance of the pristine GNS and GNS/IL composites. The cycle stability of the prepared composites was evaluated at a potential range between -0.8 V to 0.2 V at a scan rate of 100 mVs^{-1} for 3000 cycles. The GNS/IL composite electrode exhibits an excellent cycle performance (~80% of initial value for 3000 cycles), which was higher than the 45% retention of the pristine GNS.

http://dx.doi.org/10.5772/59201

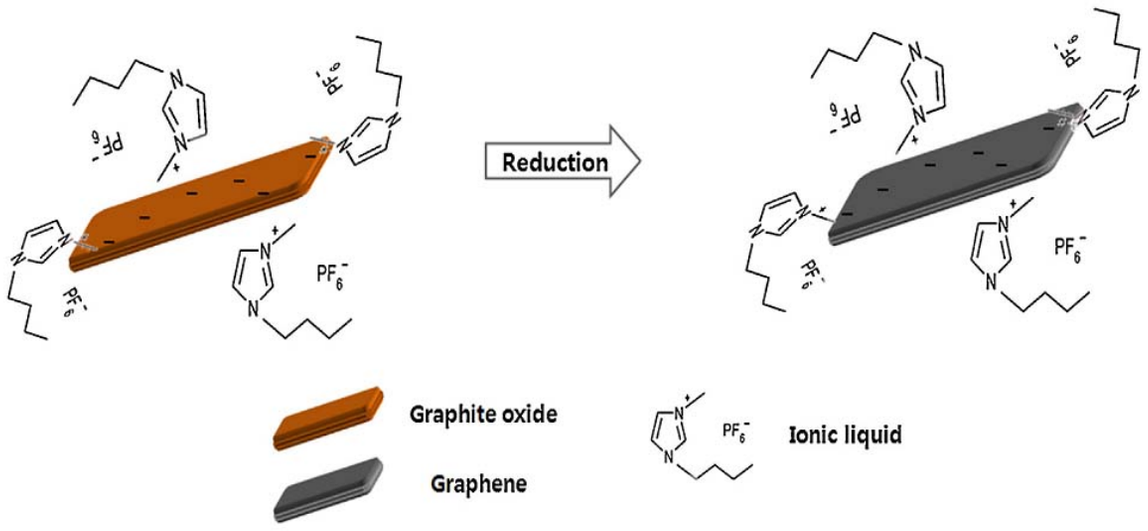

[Reproduced from [116] Kim J, Kim S. Preparation and electrochemical property of ionic liquid-attached graphene nanosheets for the application of a supercapacitor electrode. Electrochimica Acta. 2014; 119, 11– 15, Copyright (2014), with permeation from Elsevier].

Figure 13. Schematic representation of the preparation process of GNS/IL composites.

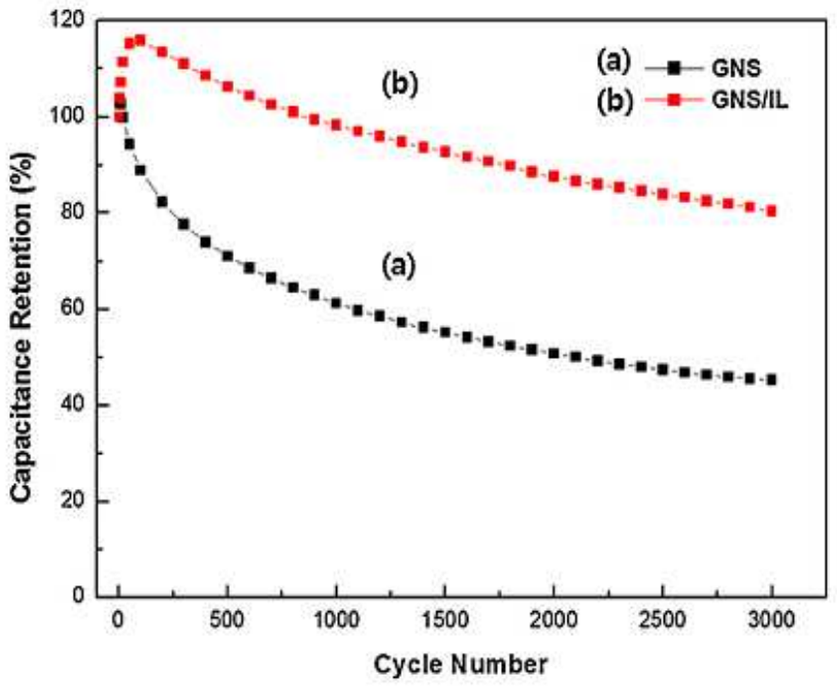

[Reproduced from [116] Kim J, Kim S. Preparation and electrochemical property of ionic liquid-attached graphene nanosheets for the application of a supercapacitor electrode. Electrochimica Acta. 2014; 119, 11– 15, Copyright (2014), with permission from Elsevier].

Figure 14. Cycling performances of pristine GNS and GNS/IL composites.

2.5.1.4. Poly ionic liquid as an electrolyte for graphene supercapacitors

Maoa et al. reported [117] a new concept of using conjugated polyfluorene imidazolium ionic liquids (PILs) intercalated reduced graphene oxide for high-performance supercapacitor electrode materials. Two polyfluorene homo-polymers (hoPIL) and co-polymers (co-PIL) carrying hexyl imidazolium bromide side chains were designed and synthesized. Their corresponding intercalated reduced graphene oxide materials, hoPIL-RGO and coPIL-RGO, exhibited good electrochemical performance in aqueous electrolytes as well as in ionic liquid electrolyte 1-butyl-3-methylimidazolium tetrafluoroborate ($BMIMBF_4$). High specific capacitances of 222 F g^{-1}at a current density of 0.2 A g^{-1} and 132 F g^{-1} at 0.5 A g^{-1} were obtained for coPIL-RGO in 6 M KOH and BMIMBF4 accordingly. When assembled into a symmetric two-electrode cell with graphene materials as electrodes and BMIMBF4/acetonitrile (1:1) as an electrolyte, an energy density of 14.7 Wh kg^{-1} was obtained for coPIL-RGO at a current density of 0.5 A g^{-1}, and a maximum power density of 347 kW kg^{-1} was achieved for hoPIL-RGO at a current density of 5 A g^{-1} with good cycling stability.

Figure 15 shows the chemical structure of conjugated polyfluorenes and their corresponding conjugated polyfluorene imidazolium ionic liquids.

Improving the electrolyte's accessibility to the surface of the carbon nanomaterials is a challenge to be overcome in supercapacitors based on ionic liquid electrolytes. Trigueiro et al. [118] report the preparation of supercapacitors based on reduced graphene oxide (RGO) electrodes and ionic liquid as the electrolyte (specifically, 1-methyl-1-propylpyrrolidinium bis(trifluoromethylsulfonyl)imide or [MPPy][TFSI]).

Two types of electrodes were compared: the RGO-based electrode and a poly(ionic liquid)-modified RGO electrode (PIL:RGO). The supercapacitor produced with the PIL:RGO electrode and [MPPy][TFSI] showed an electrochemical stability of 3 V and provided a capacitance of 71.5 F g^{-1} at room temperature; this capacitance is 130% higher with respect to the RGO-based supercapacitor. The decrease of the specific capacitance after 2000 cycles is only 10% for the PIL:RGO-based device. The results revealed the potential of the PIL:RGO material as an electrode for supercapacitors. This composite electrode increases the compatibility with the ionic liquid electrolyte compared to an RGO electrode, promoting an increase in the effective surface area of the electrode accessible to the electrolyte ions. Galvanostatic charge/discharge curves for RGO and PIL:RGO capacitors at 25 °C (current density: 0.2 A g^{-1}) are shown in figure 16.

Kim et al. [119] reported a high-performance supercapacitor incorporating a poly(ionic liquid)-modified reduced graphene oxide (PIL:RG-O) electrode and an ionic liquid (IL) electrolyte (specifically, 1-ethyl-3-methylimidazolium bis(trifluoromethylsulfonyl)amide or EMIM-NTf_2). PIL:RG-O provides enhanced compatibility with the IL electrolyte, thereby increasing the effective electrode surface area accessible to electrolyte ions. The supercapacitor assembled with PIL:RG-O electrode and EMIM-NTf_2 electrolyte showed a stable electrochemical response of up to a 3.5 V operating voltage and was capable of yielding a maximum energy density of 6.5 W h/kg with a power density of 2.4 kW/kg. These results demonstrate the potential of the PIL:RG-O material as an electrode in high-performance supercapacitors.

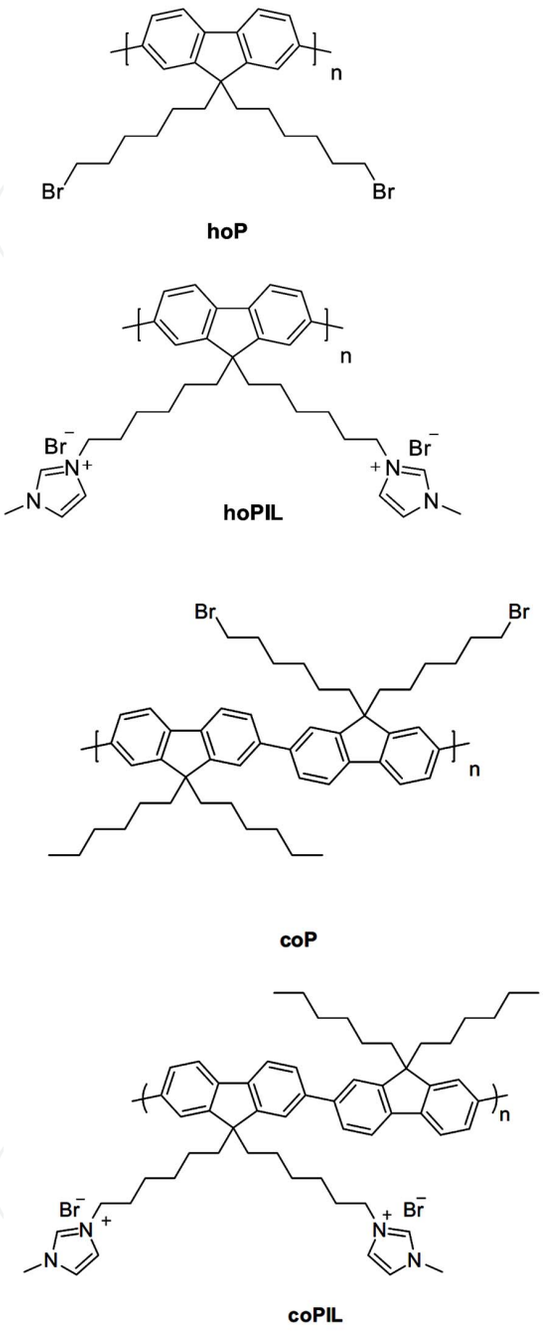

[Reprinted from [117] Maoa L, Li Y, Chi C, Chan H, Wu J. Conjugated polyfluorene imidazolium ionic liquids intercalated reduced graphene oxide for high-performance supercapacitor electrodes, Nano Energy 2014: 6, 119–128, Copyright (2014), with permission from Elsevier].

Figure 15. Chemical structure of conjugated polyfluorenes and their corresponding conjugated polyfluorene imidazolium ionic liquids.

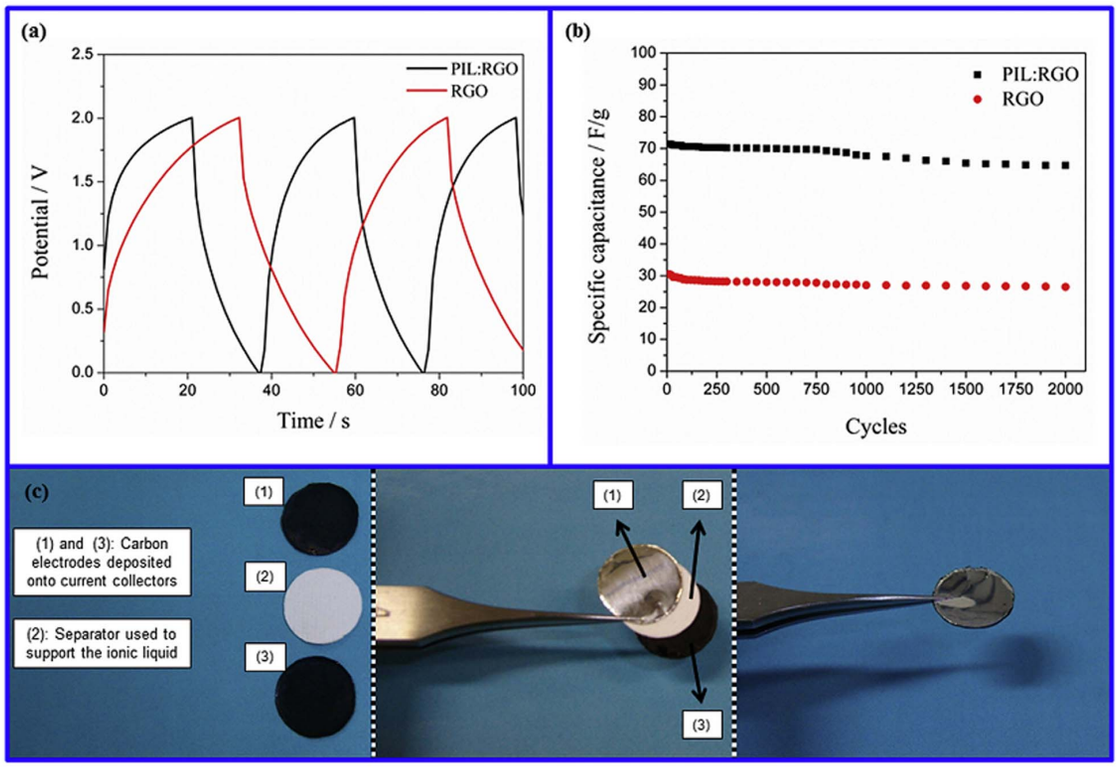

[Reprinted from [118] Trigueiro J P C, Lavall R L, Silva G G. Supercapacitors based on modified graphene electrodes with poly(ionic liquid) Journal of Power Sources.2014: 256, 264-273, Copyright (2014), with permission from Elsevier].

Figure 16. Galvanostatic charge/discharge curves for RGO and PIL:RGO capacitors at 25 °C (current density: 0.2 A g^{-1}) (a). The specific capacitance change as a function of the number of charge/discharge cycles (b). Optical images of the prototype supercapacitor developed in this work. From left to right: electrodes of carbon nanomaterials and the separator soaked with ionic liquid, the sequence used for the preparation of the device and the resulting device (c)

2.5.1.5. Miscellaneous application of ionic liquids in supercapacitors based on graphene

Beta-nickel hydroxide nanowires/reduced graphene oxide (RGO) composites are fabricated by a one-step reactable ionic liquid-assisted hydrothermal method, using the versatile 1-butyl-3-methylimidazolium trifluoroacetate as templates, co-solvents and reactants as used by Liu et al. [120]. The results show that β-$Ni(OH)_2$ nanowires are well dispersed on the surface of the reduced graphene oxide sheets, and the as-prepared β-$Ni(OH)_2$ nanowires/RGO composite exhibits a huge BET surface area of 216.99 m^2g^{-1} with a pore volume of 0.34m^3g^{-1}. Furthermore, a β-$Ni(OH)_2$ nanowires/RGO composite as an electrode material for supercapacitors displays high specific capacitance, good cycling stability and coulombic efficiency. An extremely high specific capacitance of ~1875 F g^{-1} can be obtained at 1 A g^{-1} in 6M KOH aqueous solution, and retains 98.3% of its original capacity after 1000 charge/discharge cycles at 8 A g^{-1}. The resulting composite is a promising candidate as an electrode material for extensive applications in energy storage systems.

Reduced graphene oxide (rGO)/ionic liquids (IL) composites with different weight ratios of IL to rGO were synthesized by Kim et al. [121] using a simple method. In these composites, IL contributed to the exfoliation of rGO sheets and to the improvement of the electrochemical

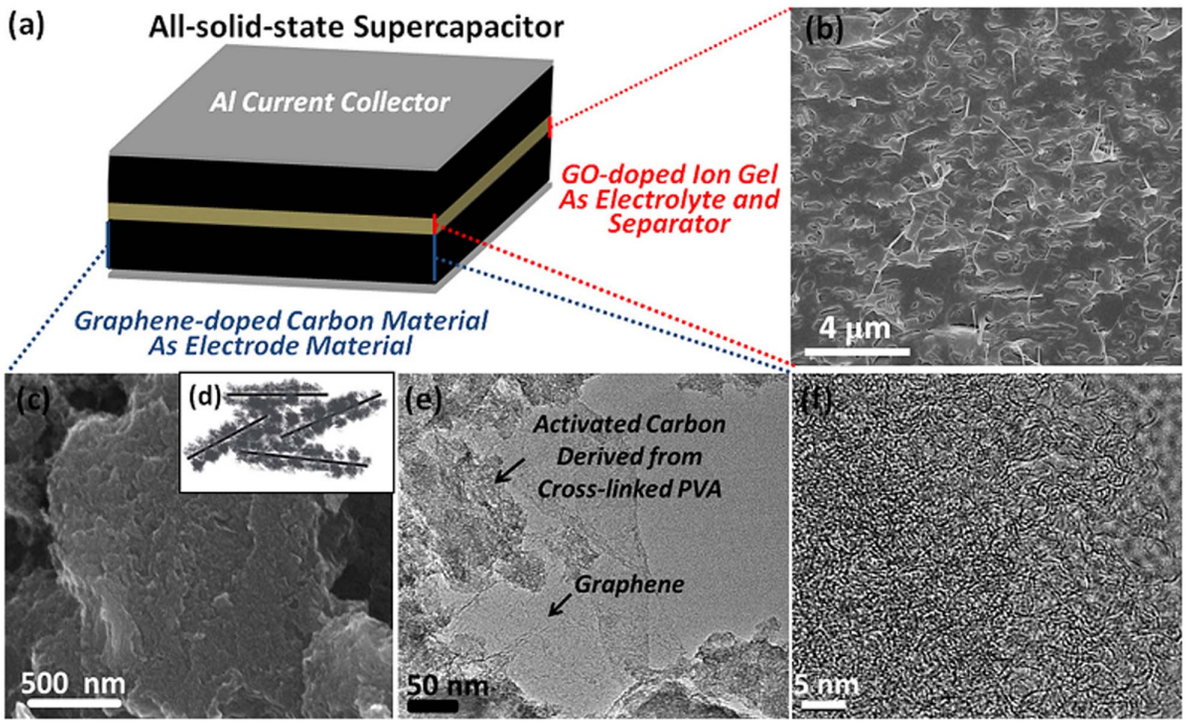

[Reproduced from [122] Yang X, Zhang L, Zhang F, Zhang T, Huang Y, Chen Y. A high-performance all-solid-state supercapacitor with graphene-doped carbon material electrodes and a graphene oxide-doped ion gel electrolyte. Carbon.2014; 72, 381 – 386, Copyright (2014), with permission from Elsevier].

Figure 17. (a) Diagram of an all-solid-state supercapacitor. (b) Low-magnification scanning electron microscopy (SEM) image of themorphology of the GO-doped ion gel. (c) SEM image of graphene-doped carbonmaterial. The activated carbon is dispersed and coated on the graphene sheets. (d) Schematic of the structure of the graphene-doped carbon material. (e) Transmission electron microscopy (TEM) image of the graphene-doped carbon material. (f) High-resolution transmission electron microscopy (HR-TEM) image of the activated carbon, coated on the graphene sheets.

properties of the resulting composites by enhancing the ion diffusion and charge transport. The TEM images showed that IL was coated on the surface of rGO in a translucent manner. The electrochemical analysis of the prepared composites was carried out by performing cyclic voltammetry (CV), galvanostatic charge/discharge, and electrochemical impedance spectroscopy (EIS). Among the prepared composites, the one with a weight ratio of rGO to IL of 1:7 showed the highest specific capacitance of $147.5 Fg^{-1}$ at a scan rate of $10 mVs^{-1}$. In addition, the rate capability and cycle performance of the composites were enhanced compared to pristine rGO. These enhanced properties make the composites suitable as electrode materials for better performance supercapacitors.

Yang et al. [122] demonstrated a high-performance all-solid-state supercapacitor with a graphene-doped carbon electrodematerial and a graphene oxide (GO)-doped ion gel as a gel polymer electrolyte and separator. The configuration of the all-solid-state supercapacitor described here is schematically shown in Figure17.

Because of the ultrahigh specific surface area ($3193 m^2 g^{-1}$), suitable pore-size distribution (primarily 1–4 nm), and excellent electrical conductivity ($67 Sm^{-1}$) of the graphene-doped carbon material, as well as the broad electrochemical window (0–3.5 V) and high ionic

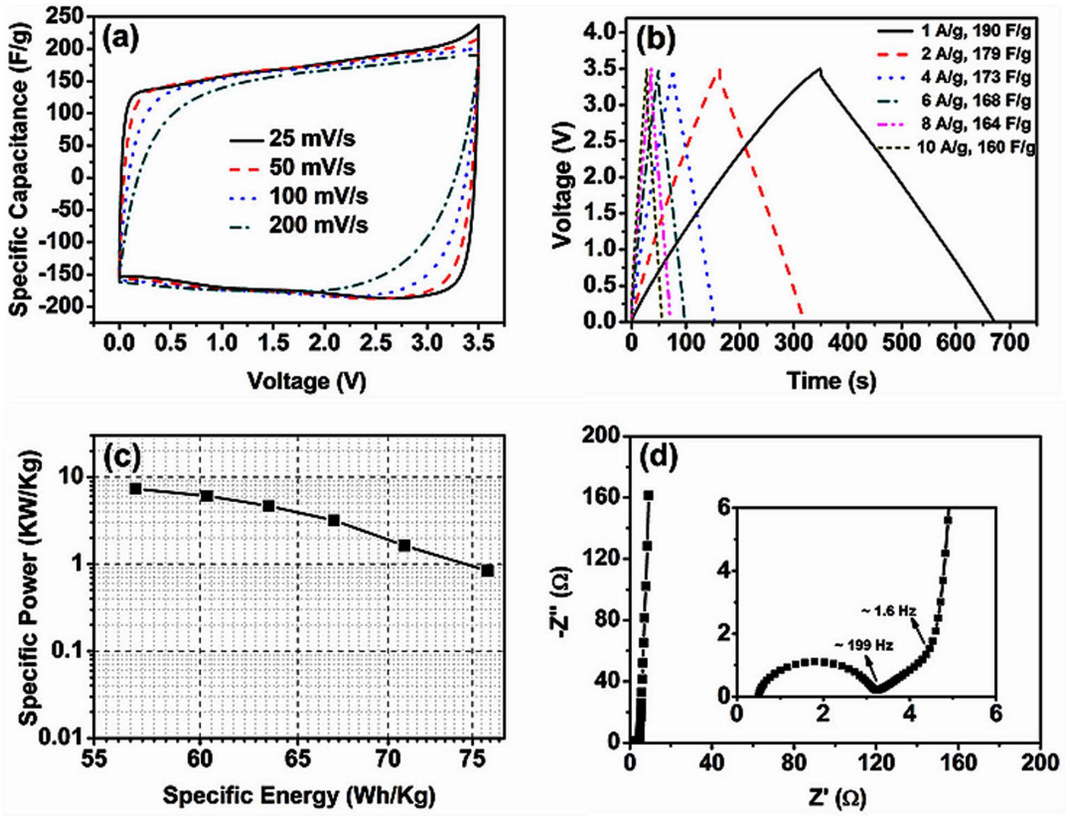

[Reproduced from [122] Yang X, Zhang L, Zhang F, Zhang T, Huang Y, Chen Y. A high-performance all-solid-state supercapacitor with graphene-doped carbon material electrodes and a graphene oxide-doped ion gel electrolyte. Carbon.2014; 72, 381 – 386, Copyright (2014), with permission from Elsevier].

Figure 18. Performance characteristics of the all-solid-state supercapacitor. (a) Cyclic voltammetry (CV) curves at various scan rates. (b) Galvanostatic charge/discharge curves under different current densities. (c) Ragone plot. (d) Nyquist impedance plots in the frequency range 10–100 kHz. The inset shows a magnified view of the high frequency region of the impedance spectra.

conductivity of the GO-doped ion gel, the all-solid-state supercapacitor demonstrates outstanding performance with a specific capacitance of 190 F g^{-1} and an energy density of 76Wh kg^{-1}at $1Ag^{-1}$, and a specific capacitance of 160 F g^{-1} and an energy density of 57Wh kg^{-1} at 10 A g^{-1}. In addition, the all-solid-state supercapacitor exhibits similar and excellent performance as does the compared conventional liquid supercapacitor with respect to specific capacitance, capacitance retention, internal resistance, and frequency response. The performance characteristics of the all-solid-state supercapacitors are shown in figure 18. Tamilarasan et al. [123] reported the fabrication of a mechanically stable, flexible grapheme-based all-solid-state supercapacitor with ionic liquid incorporated polyacrylonitrile (PAN/[BMIM][TFSI]) electrolyte for electric vehicles (EVs). The PAN/[BMIM][TFSI] electrolyte shows high ionic conductivity (2.42 mS/cm at 28 °C) with high thermal stability. The solid-like layered phase of ionic liquid is observed on the surface of the pores of the PAN membrane along with the liquid phase which made it possible to hold 400 wt% of the mobile phase. This phase formation is facilitated by the ionic interaction of C^N moieties with the electrolyte ions. A supercapacitor device, comprised of PAN/[BMIM][TFSI] electrolyte and graphene as an electrode, is fabri-

cated and the performance is demonstrated. Several parameters of the device, such as, energy storage and discharge capacity, internal power dissipation, operating temperature, safe operation and mechanical stability, meet the requirements of future EVs. In addition, a good cyclic stability is observed even after 1000 cycles.

All-solid-state thin supercapacitors were fabricated by Pandey et al. [124] using current pulse polymerized poly(3,4-ethylenedioxythiophene) (PEDOT) over carbon fibre paper and ionic liquid-based gel polymer electrolyte. The performance characteristics of the supercapacitor cells were evaluated by ac impedance spectroscopy, cyclic voltammetry and galvanostatic charge/discharge techniques. The PEDOT electrode shows the specific capacitance of w154.5 F g^{-1}, which corresponds to the cell area-normalized capacitance of 85 mF cm^{-2}. The maximum specific energy and specific power of the solid-state supercapacitor cell, calculated from charge/discharge characteristics, are 6.5 Wh kg^{-1} and 11.3 kW kg^{-1}, respectively. The solid-state supercapacitor shows good cycle durability and time stability. The thin, lightweight, gel electrolyte-based supercapacitor shows considerable potential for low-cost, high-performance energy storage applications. Cyclic voltammetry (CV) curves of the supercapacitor cell at different scan rates are shown in figure 19.

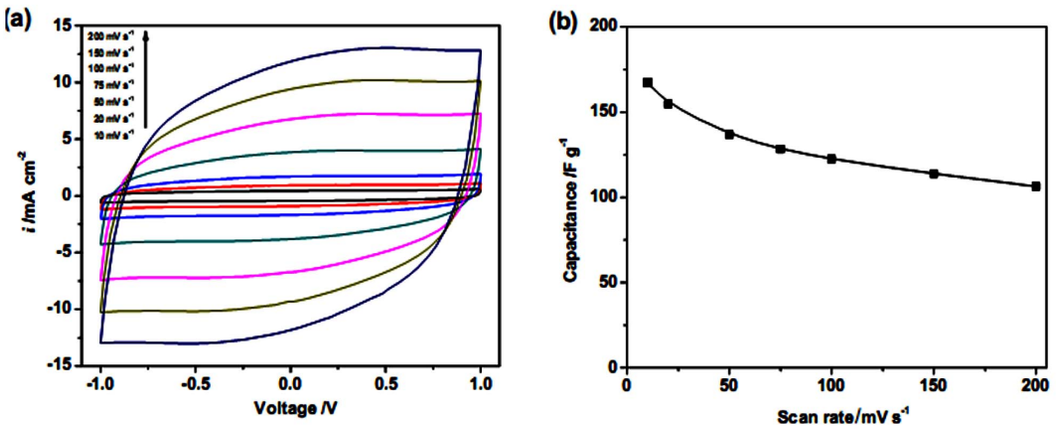

[Reproduced from [124] Pandey G P, Rastogi A C, Westgate C R. All-solid-state supercapacitors with poly(3,4-ethylenedioxythiophene)-coated carbon fiber paper electrodes and ionic liquid gel polymer electrolyte. Journal of Power Sources.2014; 245, 857-865, Copyright (2014), with permission from Elsevier].

Figure 19. (a) Cyclic voltammetry (CV) curves of supercapacitor cells at different scan rates. (b) Variation in the capacitance of the PEDOT electrode, calculated from CV curves, as a function of the scan rates.

3. Conclusions

Graphene-based materials have great potential for application in supercapacitors and other green energy devices. There has been much interest in graphene-based electronic devices because graphene provides excellent electrical, optical and mechanical properties. While the supercapacitors available today perform well, it is generally agreed that there is considerable scope for improvement (e.g., improved performance at higher frequencies). Thus, it is likely

that graphene will continue to play a principal role in supercapacitor technology, mainly through the further optimization of porosity, surface treatments to promote wettability, and reduced inter-particle contact resistance. The use of ILs as solvent-free electrolytes in supercapacitors permits a high cell voltage and is the most powerful strategy for increasing specific energy. An effective application in supercapacitors requires that ILs be designed to match wide ESWs to high conductivity and wide duty temperature. The design and synthesis of new nanostructures and architectures based on grapheme and modern ionic liquids will be an important task in the future.

Author details

Elaheh Kowsari*

Address all correspondence to: kowsarie@aut.ac.ir

Department of Chemistry, Amirkabir University of Technology, Tehran, Iran

References

[1] Zhang L L, and Zhao X S. Carbon-based materials as supercapacitor electrodes. Chem Soc Rev. 2009; 38, 2520–2531.

[2] Winter M, Brodd R J, What Are Batteries, Fuel Cells, and Supercapacitors. Chem Rev. 2004; 104, 4245–4269.

[3] Conway B E. Electrochemical Supercapacitors: Scientific Fundamentals and Technological Applications. New York, Kluwer-Plenum 2009.

[4] Burke A. Ultracapacitors: why, how, and where is the technology. Journal of Power Sources. 2000; 91(1): 37-50.

[5] Kotz R, Carlen M. Principles and applications of electrochemical capacitors. Electrochimica Acta 2000; 45, 2483-2498.

[6] Aricò A S, Bruce P, Scrosati B, Tarascon J M, Schalkwijk W V. Nanostructured materials for advanced energy conversion and storage devices. Nature Materials.2005; 4, 366-377.

[7] Sharma P, Bhatti T S. A review on electrochemical double-layer capacitors. Energy Conversion and Management 2010; 51, 2901–2912.

[8] Stoller M D, Ruoff R S. Best practice methods for determining an electrode material's performance for ultracapacitors Energy Environ Sci. 2010; 3, 1294–1301.

[9] Peng C, Zhang S, Zhou X, Chen G Z. Unequalisation of electrode capacitances for enhanced energy capacity in asymmetrical supercapacitors. Energy Environ. Sci. 2010; 3, 1499–1502.

[10] Liu C, Li F, Ma L P, Cheng H M. Advanced Materials for Energy Storage. Adv. Mater. 2010; 22, E28–E62.

[11] Frackowiak E. Carbon materials for supercapacitor application. Phys. Chem. Chem. Phys. 2007; 9, 1774–1785.

[12] Hall P J, Mirzaeian M, Fletcher S I, Sillars F B, Rennie A J R, Shitta-Bey G O, Wilson G, Cruden A, Carter R. Energy storage in electrochemical capacitors: designing functional materials to improve performance. Energy Environ Sci. 2010; 3, 1238–1251.

[13] Pumera M. Graphene-based nanomaterials for energy storage. Energy Environ. Sci. 2011; 4, 668–674.

[14] Sun Y, Wu Q, Shi G. Graphene based new energy materials. Energy Environ. Sci. 2011; 4, 1113–1132.

[15] Huang X, Zeng Z, Fan Z, Liu J, Zhang H. Graphene-Based Electrodes, Adv. Mater. 2012; 24, 6004–5979..

[16] Li Z, Luppi G, Geiger A, Josel H P, Cola L D. Bioconjugated Fluorescent Zeolite L Nanocrystals as Labels in Protein Microarrays, Small 2011; 7, 3193–3201.

[17] Zhang L L, Zhao X S. Carbon-based materials as supercapacitor electrodes. Chem Soc Rev.2009, 38, 2520–2531.

[18] Wei L, Nitta N, Yushin G. Lithographically patterned thin activated carbon films as a new technology platform for on-chip devices, ACS Nano 2013,7, 6498-6506.

[19] Wang G, Wang H, Lu X, Ling Y, Yu M, Zhai T, Tong Y, Li Y. Solid-state supercapacitor based on activated carbon cloths exhibits excellent rate capability. Adv. Mater. 2014, 26, 2676-2682.

[20] Wang D W, Li F, Liu M, Lu G Q, Cheng H M. 3D Aperiodic Hierarchical Porous Graphitic Carbon Material for High-Rate Electrochemical Capacitive Energy Storage, Angew. Chem. Int. Ed. 2008, 47, 373-376.

[21] Chmiola J, Yushin G, Gogotsi Y, Portet C, Simon P, Taberna P L. Anomalous Increase in Carbon Capacitance at Pore Sizes Less Than 1 Nanometer, Science. 2006; 313, 1760-1763.

[22] Wu X L, Wen T, Guo H L, Yang S, Wang X, Xu A W. Biomass-derived sponge-like carbonaceous hydrogels and aerogels for supercapacitors., ACS Nano 2013;7, 3589-3597.

[23] Portet C, Yushin G, Gogotsi Y. Electrochemical performance of carbon onions, nanodiamonds, carbon black and multiwalled nanotubes in electrical double layer capacitors. Carbon. 2007; 45, 2511-2518.

[24] Cheng Z, Jinping L. Carbon nanotube network film directly grown on carbon cloth for high-performance solid-state flexible supercapacitors. Nanotechnology. 2014; 25, 035402.

[25] Zheng H, Zhai T, Yu M, Xie S, Liang C, Zhao W, Wang SCI, Zhang Z, Lu X. TiO2@C core–shell nanowires for high-performance and flexible solid-state supercapacitors. J Mater Chem C 1 2013; 225-229.

[26] Swu Z S, Sun Y, Tan Y Z, Yang S, Feng X, Müllen K. Three-dimensional graphene-based macro- and mesoporous frameworks for high-performance electrochemical capacitive energy storage. J Am Chem Soc 2012; 134 19532-19535.

[27] Liu W W, Feng Y Q, Yan B X, Chen J T, Xue Q J. Superior Micro-Supercapacitors Based on Graphene Quantum Dots. Adv Funct Mater. 2013; 23, 4111-4122.

[28] Jin K Y, Haegeun C, Chi-Hwan H, Woong K. All-solid-state flexible supercapacitors based on papers coated with carbon nanotubes and ionic-liquid-based gel electrolytes, Nanotechnology. 2012; 23, 065401.

[29] Yoon S, Lee J W, Hyeon T, Oh SM. Electric Double-Layer Capacitor Performance of a New Mesoporous Carbon, J Electrochem Soc 2000; 147, 2507-2512.

[30] Chmiola J, Yushin G, Gogotsi Y, Portet C, Simon P, Taberna P L. Anomalous increase in carbon capacitance at pore sizes less than 1 nanometer. Science. 2006; 313,1760-1763.

[31] Geim A K, Novoselov K S. The rise of graphene, Nat. Mater. 2007; 6, 183–191.

[32] Li X, Cai W, An J, Kim S, Nah J, Yang D, Piner R, Velamakanni A, Jung I, Tutuc E, Banerjee S K, Colombo L, Ruoff R S. Large-Area Synthesis of High-Quality and Uniform Graphene Films on Copper Foils. Science 2009; 324, 1312–1314.

[33] Soldano C, Mahmood A, Dujardin E. Production, properties and potential of graphene. Carbon. 2010; 48, 2127–2150.

[34] Srivastava A, Galande C, Ci L, Song L, Rai C, Jariwala D, Kelly K F, Ajayan P M. Novel Liquid Precursor-Based Facile Synthesis of Large-Area Continuous, Single, and Few-Layer Graphene Films. Chem Mater 2010; 22, 3457–3461.

[35] Biswas S, Drzal L T. Multilayered Nano-Architecture of Variable Sized Graphene Nanosheets for Enhanced Supercapacitor Electrode Performance. ACS Appl Mater Interfaces 2010; 2, 2293–2300.

[36] Kim K S, Zhao Y, Jang H, Lee S Y, Kim J M, Kim K S, Ahn J H, Kim P, Choi J Y, Hong B H. Large-scale pattern growth of graphene films for stretchable transparent electrodes, Nature 2009, 457, 706–710.

[37] Wu J, Becerril H A, Bao Z, Liu Z, Chen Y, Peumans P. Organic solar cells with solution-processed graphene transparent electrodes, Appl Phys Lett. 2008; 92, 263302-263303.

[38] Becerril H A, Mao J, Liu Z, Stoltenberg R M, Bao Z, Chen Y. Evaluation of solution-processed reduced graphene oxide films as transparent conductors, ACS Nano 2008; 2, 463–470.

[39] [39] Eda G, Fanchini G, Chhowalla M. Large-area ultrathin films of reduced graphene oxide as a transparent and flexible electronic material, Nat. Nanotechnol. 2008; 3, 270–274.

[40] Kinoshita K. Carbon: Electrochemical and Physiochemical Properties. Wiley-Interscience: New York. 1988.

[41] Vivekchand S R C, Rout C S, Subrahmanyam K S, Govindaraj A, Rao C N R. Graphene-based electrochemical supercapacitors, J Chem Sci. 2008, 120,9–13.

[42] Stoller M D, Park S, Zhu Y, An J, Ruoff R S. Graphene-Based Ultracapacitors. Nano Lett. 2008, 8, 3498–3502.

[43] Wang Y, Shi Z, Huang Y, Ma Y, Wang C, Chen M, Chen Y. Supercapacitor Devices Based on Graphene Materials, J. Phys. Chem. C 2009, 113, 13103–13107.

[44] Wang D W, Li F, Wu Z S, Ren W, Cheng H-M. Electrochemical interfacial capacitance in multilayer graphene sheets: Dependence on number of stacking layers. Electrochem. Commun. 2009; 11, 1729–1732.

[45] Liu C, Yu Z, Neff D, Zhamu A, Jang B Z. Graphene-based supercapacitor with an ultrahigh energy density. Nano Lett. 2010; 10, 4863–4868.

[46] Pumera M. Graphene-based nanomaterials for energy storage, Energy Environ. Sci. 2011; 4, 668-674.

[47] Balandin A, Ghosh S, Bao W, Calizo I, Teweldebrhan D, Miao F, Lau C N. Superior Thermal Conductivity of Single-Layer Graphene, Nano Lett. 2008; 8, 902–907.

[48] Lee C, Wei X, Kysar J W, Hone J. Measurement of the Elastic Properties and Intrinsic Strength of Monolayer Graphene Science 2008; 321, 385–388.

[49] Jang B Z, Aruna Z. Processing of nanographene platelets (NGPs) and NGP nanocomposites: a review J. Mater. Sci. 2008, 43, 5092–5101.

[50] Xia J, Chen F, Li J, Tao N. Measurement of the quantum capacitance of graphene. Nat. Nanotechnol. 2009; 4, 505–509.

[51] Liu C, Yu Z, Neff D, Zhamu A, Jang B Z. Graphene-Based Supercapacitor with an Ultrahigh Energy Density. Nano Lett. 2010, 10, 4863–4868.

[52] Armand M, Endres F, MacFarlane D R, Ohno H, Scrosati B. Ionic-liquid materials for the electrochemical challenges of the future, Nat Mater 2009; ;8, 621-629.

[53] Nanjundiah C, McDevitt S F, Koch V R. Differential Capacitance Measurements in Solvent-Free Ionic Liquids at Hg and C Interfaces, J. Electrochem. Soc. 1997; 144, 3392-3397.

[54] McEwen A B, Ngo H L, Compte K L, Goldman J L. Electrochemical Properties of Imidazolium Salt Electrolytes for Electrochemical Capacitor Applications J. Electrochem. Soc. 1999; 146, 1687-1695.

[55] Balducci A, Bardi U, Caporali S, Mastragostino M, Soavi F. Ionic liquids for hybrid supercapacitors, Electrochemistry Communications 2004;6, 566–570

[56] Supercapacitor, http://en.wikipedia.org/wiki/Supercapacitor, (accessed 10 August 2014)

[57] Kotz K, Carlen M. Principles and applications of electrochemical capacitors, Electrochim Acta. 2000, 45, 2483-2498.

[58] Gouy G. The surface charge of a cell lipid membrane, J Phys, 1910; 4, 457-468.

[59] Chapman D L. A contribution to the theory of electrocapillarity. Philos. Mag. 1913; 6, 475-481.

[60] Stern O Z. Schematic of double layer in a liquid at contact with a negatively-charged solid. Electrochem. 1924; 30, 508-516.

[61] Zhang L, Zhao X S. Carbon-based materials as supercapacitor electrodes. Chem Soc Rev, 2009; 38, 2520–2531.

[62] Kurzweil P. Capacitors | Electrochemical Double-Layer Capacitors, Reference Module in Chemistry, Molecular Sciences and Chemical Engineering Encyclopedia of Electrochemical Power Sources, 2009; 607–633.

[63] Wang H, Pilon L. Mesoscale modeling of electric double layer capacitors with three-dimensional ordered structures. Journal of Power Sources, 2013; 221,252-260.

[64] Halper M S, Ellenbogen J C. Supercapacitors: A Brief Overview (Technical report, March2006)). MITRE Nanosystems Group. Retrieved 2014-01-20.

[65] Namisnyk A M. A survey of electrochemical supercapacitor technology (Technical report). Retrieved 2013-04-02.

[66] (a) Frackowiak E, Beguin F. Carbon materials for the electrochemical storage of energy in Capacitors. Carbon. 2001, 39 937–950.(b) http://en.wikipedia.org/wiki/Activated_carbon

[67] Carbide-derived-carbon. http://en.wikipedia.org/wiki.

[68] Presser V, Heon M, Gogotsi Y. Carbide-Derived Carbons – From Porous Networks to Nanotubes and Graphene. Advanced Functional Materials 2011;21 (5): 810–833.

[69] Kyotani T, Chmiola J, Gogotsi Y. Carbon Materials for Electrochemical Energy Storage Systems. CRC Press/Taylor and Francis. 2009; 77–113.

[70] Yushin G, Nikitin A, Gogotsi Y. Carbon Nanomaterials, Y. Gogotsi (ed.) CRC Taylor & Francis. 2006; 211–254.

[71] Nikitin A, Gogotsi Y. Encyclopedia of Nanoscience and Nanotechnology H.S. Nalwa(ed.), American Scientific Publishers 2004 :7 553–574.

[72] Rose M, Korenblit Y, Kockrick E, Borchardt L, Oschatz M, Kaskel S, Yushin G. Hierarchical Micro-and Mesoporous Carbide-Derived Carbon as a High-Performance Electrode Material in Supercapacitors. Small. 2011;7 (8): 1108–1117.

[73] Yeon S H, Reddington P, Gogotsi Y, Fischer J E, Vakifahmetoglu C, Colombo P. Carbide-derived-carbons with hierarchical porosity from a preceramic polymer. Carbon 2010; 48: 201–210.

[74] Presser V, Zhang L, Niu J J, McDonough J, Perez C, Fong H, Gogotsi Y. Flexible Nano-Felts of Carbide-Derived Carbon with Ultra-High Power Handling Capability. Advanced Energy Materials. 2011;1 (3): 423–430.

[75] Pandolfo A G, Hollenkamp A F. Carbon properties and their role in supercapacitors. Journal of Power Sources. 2006 157: 11–27.

[76] Arulepp M, Leis J, Lätt M, Miller F K. Rumma K, Lust E, Burke A F. The advanced carbide-derived carbon based supercapacitor. Journal of Power Sources 2006;162 (2): 1460–1466.

[77] Simon P, Gogotsi Y. Materials for electrochemical capacitors. Nature Materials 2008; 7 (11): 845–854.

[78] (a) Chmiola J, Yushin G, Gogotsi Y, Portet C, Simon P, Taberna PL. Anomalous Increase in Carbon Capacitance at Pore Sizes of Less Than 1 Nanometer. Science 2006,313 (5794): 1760–1763. (b) http://en.wikipedia.org/wiki/Carbide-derived_carbon

[79] McDonough G, Gogotsi Y. Carbon Onions: Synthesis and Electrochemical Applications, Interface. Fall. 2013; 61-66.

[80] Inagaki M, Konno H, Tanaike O. Carbon materials for electrochemical capacitors. Journal of Power Sources. 2010; 195, 7880–7903

[81] Geim A K, Novoselov K S. The rise of graphene, Nat. Mater. 2007; 6, 183–191.

[82] Li D, Kaner R B. Graphene-based materials. Science 2008; 320, 1170–1171.

[83] Westervelt R M, Graphene nanoelectronics, Science. 2008; 320; 324–325.

[84] Wu Z S, Ren W C, Xu L, Li F, Cheng H M. Doped graphene sheets as anode materials with superhigh rate and large capacity for lithium ion batteries, ACS Nano 2011;5, 5463–5471.

[85] Li Y, Chen Q, Xu K, Kaneko T, Hatakeyama R. Synthesis of graphene nanosheets from petroleum asphalt by pulsed arc discharge in water. Chemical Engineering Journal 2013; 215-216, 45–49.

[86] Sun D K, James J M. Tour, Graphene Chemistry: Synthesis and Manipulation,| J. Phys. Chem. Lett. 2011, 2, 2425–2432.

[87] Yoo J J, Balakrishnan K, Huang J, Meunier V, Sumpter B G, Srivastava A, Conway M, Reddy A L M, Jin Y, Vajtai R, Ajayan P M. Ultrathin Planar Graphene Supercapacitors, Nano Lett. 2011; 11, 1423–1427.

[88] Graphene supercapacitor breaks storage record, physicsworld.com.

[89] Liu C, Yu Z, Jang B Z, Aruna Z, Jang B Z. Graphene-Based Supercapacitor with an Ultrahigh Energy Density. Nano Letters. 2010,10 (12): 4863–4868.

[90] (a) Miller J R, Outlaw R A, Holloway B C. Graphene Double-Layer Capacitor with ac Line-Filtering Performance, Science 2010, 329 : 1637-1639.(b) http://en.wikipedia.org/wiki/Graphene

[91] Vivekchand S R C, Rout C S, Subrahmanyam K S, Govindaraj A, Rao C N R. Graphene-based electrochemical supercapacitors. J Chem Sci. 2008;120 : 9-13.

[92] Choi B G, Yang M H, Hong W H, Choi, J W, Huh Y S. 3D Macroporous Graphene Frameworks for Supercapacitors with High Energy and Power Densities. ACS Nano. 2012; 6, 4020-4028.

[93] Yoo J, Balakrishnan K, Huang J, Meunier V, Sumpter B G, Srivastava A, Conway M, Reddy A L M, Yu J, Vajtai R, Ajayan P M. Ultrathin Planar Graphene Supercapacitors. Nano Lett. 2011; 11, 1423–1427.

[94] Stoller M D, Park S, Zhu Y, An J, Ruoff R S. Graphene-Based Ultracapacitors. Nano Letters, 2008; 8(10) 3498-3502

[95] Liu C, Yu Z, Neff D, Zhamu A, Jang B Z. Graphene-Based Supercapacitor with an Ultrahigh Energy Density Nano Lett. 2010; 10, 4863–4868.

[96] Yan J, Liu J, Fan Z, Wei T, Zhang L. High-performance supercapacitor electrodes based on highly corrugated graphene sheets. Carbon. 2012; 50, 2179 – 2188.

[97] Zhang L L, Zhao X S. Carbon-based materials as supercapacitor electrodes, Chem.Soc.Rev. 2009, 38, 2520–2531.

[98] Ue M. Mobility and ionic association of lithium and quaternary ammonium salts in propylene carbonate and γ-Butyrolactone.J Electrochem Soc. 1994;141(12): 3336-3342.

[99] Arulepp M, Permann L, Leis J, Perkson A, Rumma K, Jaenes A, Lust E. Influence of the solvent properties on the characteristics of a double layer capacitor J. Power Sources. 2004; 133: 320-328.

[100] Morita M, Kaigaishi T, Yoshimoto N, Egashira M, Aida T. Effects of the Electrolyte Composition on the Electric Double-Layer Capacitance at Carbon Electrodes. Electrochem. Solid State Lett. 2006; 9(8): A386-A389

[101] Lust E, Nurk G, Jaenes A, Arulepp M, Nigu P, Moeller P, Kallip S, Sammelselg V. Electrochemical properties of nanoporous carbon electrodes in various nonaqueous electrolytes. J Solid State Electrochem.2003; 7 :91-105.

[102] Mastragostino M, Soavi F. Electrochemical Capacitors: Ionic Liquid Electrolytes, Reference Module in Chemistry. Molecular Sciences and Chemical Engineering. 2009; 649–657.

[103] Anouti M, Couadou E, Timperman L, Galiano H. Protic ionic liquid as electrolyte for high-densities electrochemical double layer capacitors with activated carbon electrode material. Electrochimica Acta.2012; 64, 110–117.

[104] Balducci A, Dugas R, Taberna P L, Simon P, Plee D, Mastragostino M, Passerini S. High temperature carbon–carbon supercapacitor using ionic liquid as electrolyte. Journal of Power Sources. 2007; 165 (2):922-927.

[105] Brandt A, Pires J, Anouti M, Balducci A. An investigation about the cycling stability of supercapacitors containing protic ionic liquids as electrolyte components. Electrochimica Acta. 2013,108, 226– 231.

[106] Coadou E, Timperman L, Jacquemin J, Galiano H, Hardacre C, Anouti M. Comparative Study on Performances of Trimethyl-Sulfonium and Trimethyl-Ammonium Based Ionic Liquids in Molecular Solvents as Electrolyte for Electrochemical Double Layer Capacitors. Phys. Chem. C, 2013, 117 (20): 10315–10325.

[107] Lu W, Hartman R. Nanocomposite Electrodes for High-Performance Supercapacitors. J.Phys.Chem.Lett. 2011, 2, 655–660

[108] Zhao D, Zhao Y, Zhang X, Xu C, Peng Y, Li H, Yang Z. Application of high-performance MnO2 nanocomposite electrodes in ionic liquid hybrid supercapacitors. Materials Letters.2013, 107: 115–118

[109] Biso M, Mastragostino M, Montaninob M, Passerinib S, Soavi F. Electropolymerization of poly(3-methylthiophene) in pyrrolidinium-based ionic liquids for hybrid supercapacitors. Electrochimica Acta.2008; 53, 7967–7971.

[110] Birbilis N, Bouzek K, Bultel Y, Cuesta A, Ferapontova E, Hartl F, Hebert K, Jones DJ, Komaba S, Kuhn A, Hantel M M, Płatek A, Kaspar T R, Nesper R, Wokaun A, Kötz R. Investigation of diluted ionic liquid 1-ethyl-3-methyl-imidazolium tetrafluoroborate electrolytes for intercalation-like electrodes use supercapacitors Electrochimica Acta 2013;110, 234–239.

[111] Tamilarasan P, Ramaprabhu S. Graphene based all-solid-state supercapacitors with ionic liquid incorporated polyacrylonitrile electrolyte, Energy.2013; 51, 374-381.

[112] Chen Y, Zhang X, Zhang D, Ma Y. High power density of graphene-based supercapacitors in ionic liquid electrolytes. Materials Letters. 2012; 68, 475–477.

[113] Tsai W Y, Lin R, Murali S, Zhang L L, McDonough J K, Ruoff R S, Taberna P L, Gogotsid Y, Simon P. Outstanding performance of activated graphene based supercapacitors in ionic liquid electrolyte from-50 to 80 °C, Nano Energy. 2013; 2, 403–411.

[114] Wei D, Ng T W. Application of novel room temperature ionic liquids in flexible supercapacitors, Electrochemistry Communications.2009; 11, 1996–1999.

[115] Chatterjee S, Rachel Carter R, Oakes L, Erwin W R, Bardhan R, Pint C L. Electrochemical and Corrosion Stability of Nanostructured Silicon by Graphene Coatings: Toward High Power Porous Silicon Supercapacitors. J. Phys. Chem. C, 2014, 118 (20), pp 10893–10902.

[116] Kim J, Kim S. Preparation and electrochemical property of ionic liquid-attached graphene nanosheets for an application of supercapacitor electrode. Electrochimica Acta. 2014; 119, 11–15.

[117] Maoa L, Li Y, Chi C, Chan H, Wu J. Conjugated polyfluorene imidazolium ionic liquids intercalated reduced graphene oxide for high performance supercapacitor electrodes. Nano Energy.2014; 6, 119–128.

[118] Trigueiro J P C, Lavall R L, Silva G G. Supercapacitors based on modified graphene electrodes with poly(ionic liquid). Journal of Power Sources. 2014; 256, 264-273.

[119] Kim T Y, Lee H W, Stoller M, Dreyer D R, Bielawski C W, Ruoff R S, Suh K S. High-performance supercapacitors based on poly(ionic liquid)-modified graphene electrodes. ACS Nano, 2011; 5 (1): 436–442.

[120] Liu W, Ju C, Jiang D, Xu L, Mao H, Wang K. Ionic liquid-assisted grown of beta-nickel hydroxide nanowires on reduced graphene oxide for high-performance supercapacitors. Electrochimica Acta. 2014,143:135-142.

[121] Kim J, Kim S. Surface-modified reduced graphene oxide electrodes for capacitors by ionic liquids and their electrochemical properties. Applied Surface Science. 2014; 295, 31–37.

[122] Yang X, Zhang L, Zhang F, Zhang T, Huang Y, Chen Y. A high-performance all-solid-state supercapacitor with graphene-doped carbon material electrodes and a graphene oxide-doped ion gel electrolyte. Carbon.2014; 72,381 – 386.

[123] Tamilarasan P, Ramaprabhu S. Graphene based all-solid-state supercapacitors with ionic liquid incorporated polyacrylonitrile electrolyte. Energy 2013; 51, 374-381.

[124] Pandey G P, Rastogi A C, Westgate C R. All-solid-state supercapacitors with poly(3,4-ethylenedioxythiophene)-coated carbon fiber paper electrodes and ionic liquid gel polymer electrolyte. Journal of Power Sources.2014; 245, 857-865